2009

Moving bed granular filtration of fast pyrolysis char: granular flow rate study

Ibrahim Adnan El-hedok
Iowa State University

Moving bed granular filtration of fast pyrolysis char: granular flow rate study

by

Ibrahim Adnan El-Hedok

A thesis submitted to the graduate faculty

in partial fulfillment of the requirements for the degree of

MASTER OF SCIENCE

Co-majors: Chemical Engineering; Biorenewable Resources and Technology

Program of Study Committee:
Robert C. Brown, Major Professor
Eric Cochran
Theodore Heindel

Iowa State University

Ames, Iowa

2009

Table of Contents

LIST OF FIGURES

LIST OF TABLES

ACKNOWLEDGEMENTS

I would like to express my great pleasure to Dr. Robert Brown for giving me the opportunity to be part of his research group and the Center for Sustainable Environmental Technologies (CSET). Indeed, it was a very rewarding experience to work with and learn from group members about the different thermochemical technologies researched. I would like to thank Dr. Brown personally for providing the support needed to complete this project and for his hard work in keeping CSET achieve higher goals. Also, I would like to thank him for his wise guidance on professional and personal matters.

I want to thank Dr. Sam Jones for providing guidance and motivation, especially at the beginning of my research when I struggled in starting and had no clear end in sight. I would like to deeply thank my colleague Lysle Whitmer for working with me on setting the experiment and for the countless discussions that made this research enjoyable. His technical intellect helped us solve many of the problems we faced, indeed without his support the project would have not been completed on time. I also extend my appreciation to all CSET students for providing any assistance and taking interest in my research.

I would like to sincerely thank my wife Ihsan Zaatari for her love, support and motivation during the frustrating times, and for her understanding when I had to work overtime and weekends. I would like to thank my parents and family for their support and encouragement to continue my education.

Finally, I want to express my appreciation to Dr. Eric Cochran and Dr. Theodore Heindel for serving on my program of study committee. I would like also to thank ConocoPhillips for providing generous funding for this research.

ABSTRACT

Moving bed granular filter (MBGF) shows a good promise for hot gas clean up of biomass fast pyrolysis to filter fine char particles. This research project examines the effect of granular flow rate on the performance of a MBGF at cold flow conditions.

In understanding the effect of granular flow rate on the MBGF performance, the filter's collection efficiency and char accumulation in the filter's are assessed at experiments of different granular residence times (t_g). A process particle counter (PPC) is used to measure the filter's exiting particle concentration, knowing the inlet concentration values the collection efficiency can be calculated. Moreover, pressure drop measurement was used as a tool to assess char accumulation in the filter. For this purpose, pressure was measured in several locations within the filter's bed in order to evaluate dust accumulation level for each bed section. A correlation of pressure drop and accumulation of char dust has been developed and used to understand how char accumulates over time for the different bed regions.

Experiments indicate that the MBGF needs to be operated below a critical granular residence time (t_g*), below which the filtration efficiency exceeds 99%. Operating above than t_g* would cause the filter to "clog" and face decrease in efficiency. The filter is found to accumulate most of the dust at the interfacial region where dust-laden gas first meets the granular media. It was also found that the interfacial region is more efficient than the other bed regions.

Decreasing the granular residence time in the filter can be used to minimize the amount of accumulated char dust in the filter, which is advantageous for avoiding secondary reactions during fast pyrolysis' hot gas filtration.

CHAPTER 1. INTRODUCTION

The growing energy demand and increasing fuel prices has led the United States to pass the new Energy Policy Act of 2005 [1]. One of the goals of this policy is to provide incentives toward utilizing clean renewable energy, such as solar, wind or biomass. Biomass, defined as any biological material that can be converted to fuel, is considered a prominent bio-renewable resource for energy. Currently two main biomass conversion technologies are heavily researched: biochemical and thermochemical [2]. Both technologies face many challenges that are yet to be met. Thermochemical conversion technologies convert biomass to fuels, chemicals, and electricity using gasification and pyrolysis technologies [2]. Gasification—partially combusting biomass in the presence of lean air—produces volatile gases such as methane, hydrogen, carbon monoxide and carbon dioxide, known as syngas. Pyrolysis—heating biomass in an oxygen free environment—produce pyrolysis oil, known as bio-oil. Both syngas and bio-oil can be converted to other valuable fuels and chemicals.

Both processes, gasification and pyrolysis, would present a high concentration of char particulates in the gases products. It is believed that the particulate matter in the fast pyrolysis process catalyze the polymerization of bio-oil, which increases the viscosity of bio-oil over time [3]. Moreover the presence of char particulate matter in the gasification effluent gaseous stream erodes components used for thermal energy conversion, such as turbine blades and heat exchangers.

Several types of filters can be used for this purpose. Cyclones can remove significant amount of char particulates. However, cyclones are inefficient in filtering smaller particles. Barrier type filters, e.g. bag-house [4] and ceramic candle filters [5], could be efficient in

filtering smaller particles, however they exhibit unsteady operation due to the need to clean the filtration surface cyclically. Moving bed granular filter (MBGF) has overcome these challenges through its continuous removal of filtration media, such as gravel or sand. Moreover, this mechanism also allows the filter to operate at low pressure drop [6].

MBGF has been designed and studied by many researchers [7], it was originally designed for the coal power industry. In 2000 Brown and co-workers at Iowa State University designed and constructed a MBGF to serve as a filter for hot gas streams, which was subsequently reported in several publications [6, 8-10]. Ritzert [9] found that 86% of filtration occurs at the interface where the gas first contacts the granules creating dust cake. The dust cake, known as "filter cake" enhances filtration by decreasing pore sizes [6, 11]. However, during actual hot pyrolysis gas filtration, the filter cake can react with the hot gases leading to "coking" or secondary reaction. Hence, it is desired to have minimum residence of char within the filter bed by withdrawing the granular media faster.

The goal of this thesis is to investigate the effect granular flow rates on char accumulation within the filter and collection efficiency. The working hypothesis is that the MBGF needs to be operated above a critical granular withdrawal rate for the filter to maintain steady state. In order to examine char collection, this study inspects pressure drop at several locations within the filter bed allowing us to locate regimes where char accumulates. The results of this study shall provide an understanding of char accumulation inside the filter, as well as to selectively operate the filter at steady state along with high efficiency.

CHAPTER 2. BACKGROUND AND LITERATURE REVIEW

2.1 Thermochemical Processing of Biomass

Biomass is any form of organic matter containing stored chemical energy which is harvested with the intent of being converted to thermal energy, electrical energy or perhaps both. Several different techniques have been employed historically to convert solid biomass fuels into more useful forms such as liquids and gasses.

Fast pyrolysis is a process which can be used to convert solid biomass fuels into oils. In pyrolysis, solid fuels are heated up to 500°C in an oxygen free environment. The external heat supply is necessary to encourage the endothermic reactions which yield different types of oil and gases. The produced oil, called bio-oil, has similar properties to crude oil which could be further refined into different possible products. Yet this bio-oil faces several challenges in utilizing and refining due to its mixture complexity and low chemical stability [2]. It is believed that the particulate matter in the fast pyrolysis process catalyze the polymerization of bio-oil, which increases the viscosity of bio-oil over time [3].

Gasification is another process which produces mainly a gaseous product called producer gas and can be used as a replacement for natural gas or upgraded to make syngas. In gasification, the solid fuels are partially combusted in the presence of lean air at a high temperature 800-1000°C. The producer gas consists of volatile gases such as methane, ethane, hydrogen, carbon dioxide and carbon monoxide. Byproducts of the gasification, which lowers the process efficiency, are tars and char [2]. Moreover the presence of char particulate matter in gasification effluent gaseous stream, used in power production, erodes

components used for thermal energy conversion such as turbine blades and heat exchangers [10].

2.2 Filtration requirement and equipment

Both processes, gasification and pyrolysis, result in high concentration of char particulates in the exiting gases from the reactor. Char particulates are commonly removed using cyclones. The removal efficiency of the cyclones can exceed 90%, however the smaller particulates typically in the range of 1-30 μm are less efficiently removed by the cyclones. Efficiencies exceeding 99% for particles less than 30 μm in size are required for many of the desired syngas and bio-oil applications.

In the case of pyrolysis, particulate filtration has to be performed before the condensation of vapors to bio-oil below 350°C [2]. Moreover, in the case of gasification it would be of thermodynamic advantage if the particulate matter was removed before passing through turbines. This necessitates the use of filtering equipment that can handle high temperatures (above 350°C). Another issue is that the filters should prevent the condensation of tars and formation of secondary char, which is known to occur when the hot gas product effluent reacts with the collected char on the filter surface [8].

Ceramic candle filter is known to be used in the industry as barrier-type hot gas filter. Typically these filters consist of ceramic porous media supporting a thin membrane. The filtration particle efficiency is determined by the choosing the pore size of the membrane pores [12]. The disadvantage of barrier-type equipments is unsteady operation due to the need to clean the filtration interface regularly. Besides ceramic candle filters faces physical damage due to thermal shock and mechanical strength degradation from temperature and

flow rate cycling [13]. Another barrier type filter is bag-house or fabric filter, which uses fine mesh fabrics to capture and retain particulate matter from gas streams. These filters face the same disadvantages as the ceramic candle filters, they need to be regenerated regularly and they have unsteady pressure drop across the media during operation.

Moving bed granular filter (MBGF) consist of filtering media, typically gravel or sand, which is withdrawn from the filter continuously to replace dirty granules with clean ones. Such configuration allows the filter to be operated continuously. The removal of the granular filter media prevents the accumulation of particulate matter inside the bed, thus eliminating the increase in pressure drop over time. The removed granules can be cleaned, recycled or simply discarded.

The granular flow in MBGF is typically downward aided by gravity and controlled at the bottom by a rotating auger or a moving belt [7]. MBGF designs differ in how the dust-laden gas enters and pass through the filter. Generally there are three designs; cross-flow as shown in **Figure 1**, co-current and counter-current as shown in **Figure 2**.

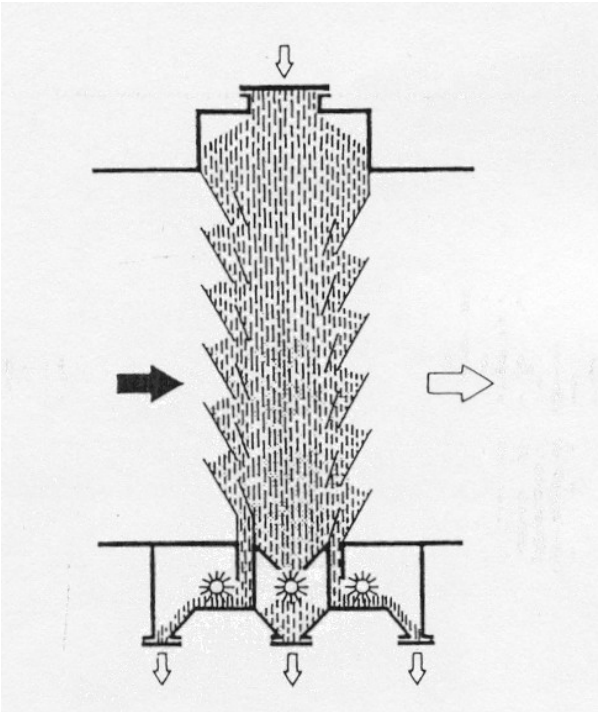

Figure 1: Cross-flow moving bed filter [14]

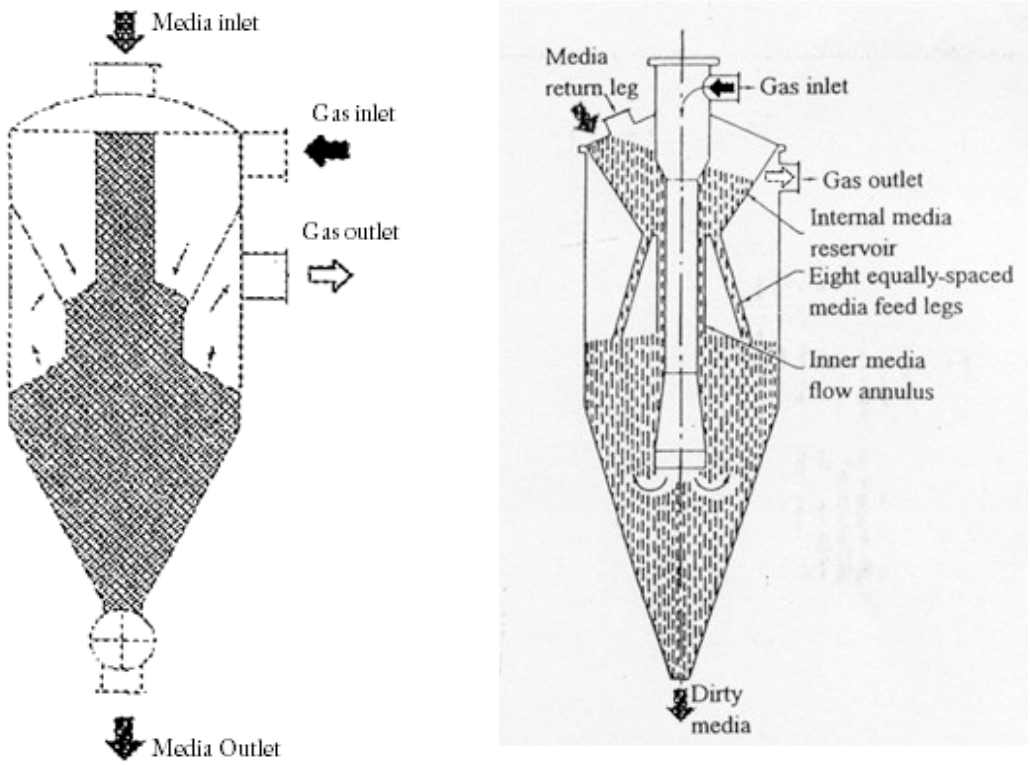

Figure 2: Co-current (left) [7], counter-current (right) [13] moving bed filters

The multiple designs of moving bed granular filters have their own advantages and disadvantages. Each design is suited for an application type to take advantage of flow properties or particle interactions in order to reach higher efficiencies. For instance, the cross-flow MBGF are suited for cases when gas passage through the granular media needs to be minimal, which has the advantage of low pressure drop. However, cross-flow MBGF posses difficulty in maintaining uniform granular flow due to impediment of louvered walls [7].

While co-current and counter-current design are similar with regard to granular flow, the major different lies in how gas interacts with the granular media. In a co-current MBGF the highest dust concentration gas meets the cleanest granules and the cleanest gas exits with the dirtiest granules. Such configuration sets a limiting factor on the overall efficiency. On the other hand, in a counter-current MBGF the dirtiest gas passes through the most dust-laden granules, while the cleanest gas meet with the cleanest granules, resulting in effectiveness similar to that of a heat exchanger.

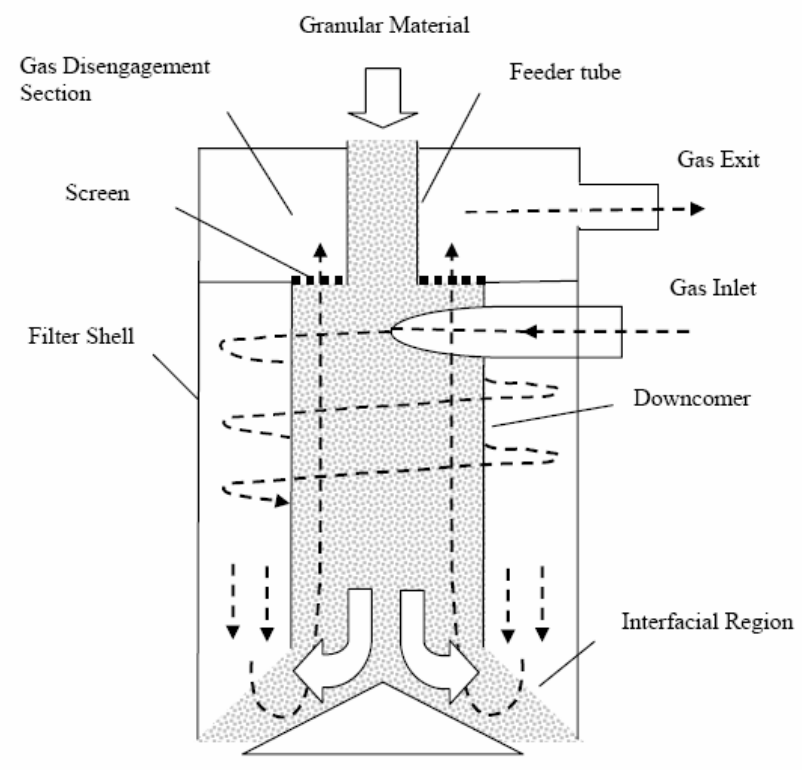

Figure 3: Moving Bed Granular Filter operating principle [15]

The counter-current MBGF design used in this research, as shown schematically in **Figure 3**, employs the formation of a dust cake layer at the interface of the gas and filtration media. This region is designated as the "Interfacial Region", which is where most of the dust collection occurs [8-10]. There are two advantages of the interfacial filtration; the first is that dust cake formation improves filtration efficiency [6, 11]. The other advantage is the better ability to minimize the dust residence time compared to the other MBGF designs. In the case of fast pyrolysis hot gas filtration, this is a great advantage that could prevent secondary reactions between collected dust and gases.

MBGF can be operated at high temperatures and pressures, proving a great economic advantage over barrier filters. Despite all the advantages the MBGF has, operating and

controlling the MBGF is a challenging task. Its collection efficiency is greatly depending on the granular properties and flow rates. The MBGF needs to be evaluated to determine the operating conditions that are best suited for type of dust and desired level of filtration.

2.2.1 Principles and mechanism of granular bed media

The filtration performance of a granular bed filter is expressed as the particle collection efficiency (η), which is the weight ratio of the dust removed by the filter to the dust entering the filter [16].

$$\eta(\%) = \frac{m_{in} - m_{out}}{m_{in}} \times 100 \qquad \text{Equation (1)}$$

Where m_{in} is mass of dust entering the filer, and m_{out} is the mass of dust exiting the filter.

Another way of expressing filtration performance is penetration (p), which is the mass percentage of particles that penetrate the full depth of a filter. This term is particularly useful when filtration efficiency (η) is very high, e.g. around 99%.

$$p(\%) = 1 - \eta(\%) \qquad \text{Equation (2)}$$

Six main mechanisms have been proposed for dust collection on the granular surface [16]. They are inertial impaction, interception, diffusion, straining, sedimentation, and electrostatic force. **Figure 4** displays the first three of the five main mechanisms of filtration.

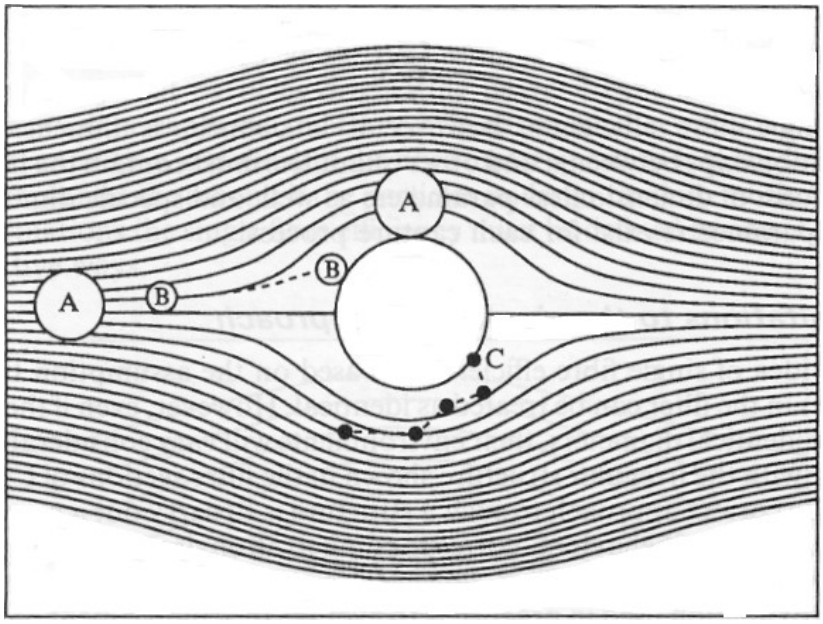

Figure 4: Mechanisms of deposition A. Interception B. Inertial impaction C. Diffusion [17]

1. Inertial Impaction

Inertial impaction is the main mechanism for particle collection on granule surface for particle above 1 μm. Consider fluid flowing around a granule, see **Figure 4**. Initially the particles follow the streamlines of the fluid flow, but as the fluid flow diverges, to avoid the granule, some of the particles, because of their inertia, tend to differentiate from their respective streamline and hit the granule surface. Thus by this diversion from the corresponding streamline, particles are deposited on the granule collector surface. The effects of inertial impaction can be characterized by the dimensionless Stokes number [16].

$$St = \frac{2\rho_p R_p^2 U C_s}{9\mu R_g} \qquad \text{Equation (3)}$$

where ρ_p is particle density, R_p is particle radius, U is superficial velocity, C_s is Cunningham factor for molecular slip, μ is gas viscosity, and R_g is granule radius.

The superficial velocity is the gas velocity, and can be calculated from the volumetric flow rate divided by the cross-sectional area of the pipe through which the gas is flowing. Cunningham factor is defined, according to Millikan's formula [18], as:

$$C_s = 1 + \frac{l}{R_p}\left[1.23 + 0.41\exp(-0.88R_p / l)\right] \qquad \text{Equation (4)}$$

where l is the mean free path of the entraining gas molecules and is given as:

$$l = \frac{\mu}{\sqrt{2P\rho/\pi}} \qquad \text{Equation (5)}$$

where P is the pressure of the gas and ρ is the gas density. Generally around normal pressure and temperature, C_s is ~1.16 [16].

Filtration due to inertial impaction is found to increase proportionally with Stokes number. Particles of St >> 1.0 [18] tend to continue on a straight line path as fluid turns around the obstacle, whereas particles of St << 1.0 would follow the fluid streamline. At high superficial gas velocities inertial impaction becomes very important.

2. Particle Interception

Interception occurs when the particle is collected by the granule surface while the particle moves along the streamline. When the dust particle radius is greater than the distance between the granular surface and the streamline, the dust particle makes contact with the granule and is removed from the flow. This collection mechanism is characterized by the

dimensionless Interception number (R) and is defined as the ratio of dust particle diameter to collector granule diameter [19]:

$$R = \frac{R_p}{R_g} \qquad \text{Equation (6)}$$

Interception becomes unimportant in the existence of external forces like inertial impaction, which is the case in most gas-granule filtration.

3. Particle Diffusion

Diffusion occurs due to the concentration gradient of particles between the fluid and the granule collector surface. The diffusion results from Brownian motion, and is valid for submicron particles [16], or Stokes number less than St<0.1.

4. Particle Straining

Particle straining occurs when the particulate to be collected is larger in size than the interstitial pores in the granular bed [16]. This mechanism is commonly used in fabric filters and ceramic candle filters. Particles that are larger than the holes size will be strained from continuing with the flow.

5. Particle Sedimentation

Sedimentation occurs when the particle is pulled down by gravity force, this might occur when the gravitational force is larger than other forces acting on the particle, e.g. drag force. A gravitational dimensionless parameter N_g is used to characterize this collection mechanism [7].

$$N_g = \frac{2.d_p{}^2 g(\rho_p - \rho)}{9\mu U}$$ Equation (7)

The condition for this mechanism is that the density of the particle is larger than that of the gas. This mechanism is important for very large particles and when superficial velocity is low, which is when N_g is larger than 10^{-3} [16].

6. Particle Deposition by Electrostatic Forces

The existence of charge on the particles or collectors or both induces attraction or repulsion between them, depending on whether they have a like or unlike charges [18]. When the granular collectors are moving relative to the particles this might generate electrostatic force which enhances filtration. Zevenhoven [20] has studied the effects of electrostatic forces on the MBGF, he asserts that the application of electrostatic forces work well for particles less than 2 μm.

Flagan et al. [21] states that inertial impaction and interception mechanisms are important for particle sizes larger than 1 μm, while for diffusion mechanism is important for particles of submicron particles. In this research, since the majority of particle sizes are larger than 1 μm, inertial impaction and interception are the most important mechanisms in describing the granular collection.

2.2.2 Factors affecting the performance of the MBGF

The moving bed granular filter has many operating factors that contribute to its collection efficiency. Some of them are: superficial velocity, granular flow rate, dust feed rate, properties of gas and dust, granule types and size [13].

Superficial velocity is the velocity of gas flow passing through the filtration bed cross section. The issue of velocity dependence is found controversial in the literature, some researchers have found that increasing the superficial velocity increases filtration efficiency [22], while others have found the opposite [23-25]. A study in 2002 by Soo [8] showed less significant effect of the gas velocity on filtration efficiency. The MBGF used by Soo is similar in design and granular material to the MBGF used in this study.

The granular flow rate (GR) is the rate at which granules are withdrawn from the MBGF. Soo have concluded that filtration efficiency improves with granular flow rate. On the other hand, some studies have found that increasing GR decreases filtration efficiency [25, 26]. Moreover, another study by Yang et al. [24] concluded that there is little significance of GR on filtration efficiency. Soo [8] have found that pressure drop decreases with higher GR. The difference in the reported literature is due to the different filter geometries and studied granular rate ranges. Some moving bed filters have more uniform granular flow due to their geometrical configuration, which leads to a better filtration [7]. On the other hand, operating the MBGF at high granular rates would create more granular interactions causing dust re-entrainment [22, 25]. It has been reported that smaller granule size increases pressure drop and efficiency [9, 25].

An increase in dust feed rate, is also controversial in the literature. Some researchers [6, 11] assert that the buildup of a layer of dust at the gas-granular interface, known as filter cake, improves collection efficiency by decreasing pore size.

The difference in the above literature could be attributed to the significant difference in the geometry of the filters, flow orientation (i.e. co-current or counter-current), dust type and particle distribution, and granular size.

A MBGF patent review in 2005 [7] concluded that the design of a moving bed should avoid granular stagnant zones that form at louvered sections. The MBGF used in this study has a dividing central cone at the bottom to direct the granular flow and reduce stagnation at the interfacial region. A study by Kuo [27] asserts that granular quasi-stagnant zones at the interfacial louvered walls leads to increasing pressure drop, due to the slow refreshing rate of granules at this region. One the other hand, Kuo states that very high granular refreshing rate may lower the overall collection efficiency of the filter. Kuo claims that the granular flow rate and granular stagnation should be selected at an optimum between filtration efficiency and pressure drop.

In the case of hot gas filtration for the fast pyrolysis process, granular stagnation inside the MBGF would be in disadvantage due to the secondary reactions that occur between the collected char and the hot gas. Hence it would be desired to have a uniform granular plug flow along with high efficiency.

Ritzert [9] used a model to help analyze the performance of the MBGF. The model showed that 86% of the filtration occurred at the interfacial region. This result was obtained by extrapolating efficiency results from changing the bed height of the MBGF. Ritzert's experiments were performed in a cold flow testing with fly ash as a model compound. A

comparison between fly ash and oak char shows that fly ash has higher filtration (~97%) efficiency than oak char (~72%). Such efficiencies were obtained using 2 mm size granules at a granular flow rate of 16.4 kg/hr. The char feed rate was 0.4 kg/hr with a particle size range of 5-300 μm. Ritzert states that the difference in efficiency between fly ash and oak char is attributed to the significant difference in density and particle shape. Ash is around five times denser than char. Moreover ash has a spherical and regular shape while char has a fibrous and irregular structure, which could induce re-entrainment of the char particles into gas stream due to higher drag force.

Huisenga [10] has worked on the same MBGF studied earlier by Ritzert. Huisenga performed cold flow and hot flow filtration experiments of pyrolysis char. The cold flow tests showed efficiencies above 98%, while hot flow tests at 400°C showed lower efficiencies below 90%. Huisenga concluded that filtration efficiency is lower for small particles less than 26 μm.

CHAPTER 3. EXPERIMENTAL METHOD

3.1 Experimental objective

This study is carried on a MBGF that was originally designed for hot gas filtration [11]. **Figure 5** shows the schematic drawing of the MBGF. This system was the subject of several previous students; Soo [8], Shi [6], Ritzert [9] and Huisenga [10].

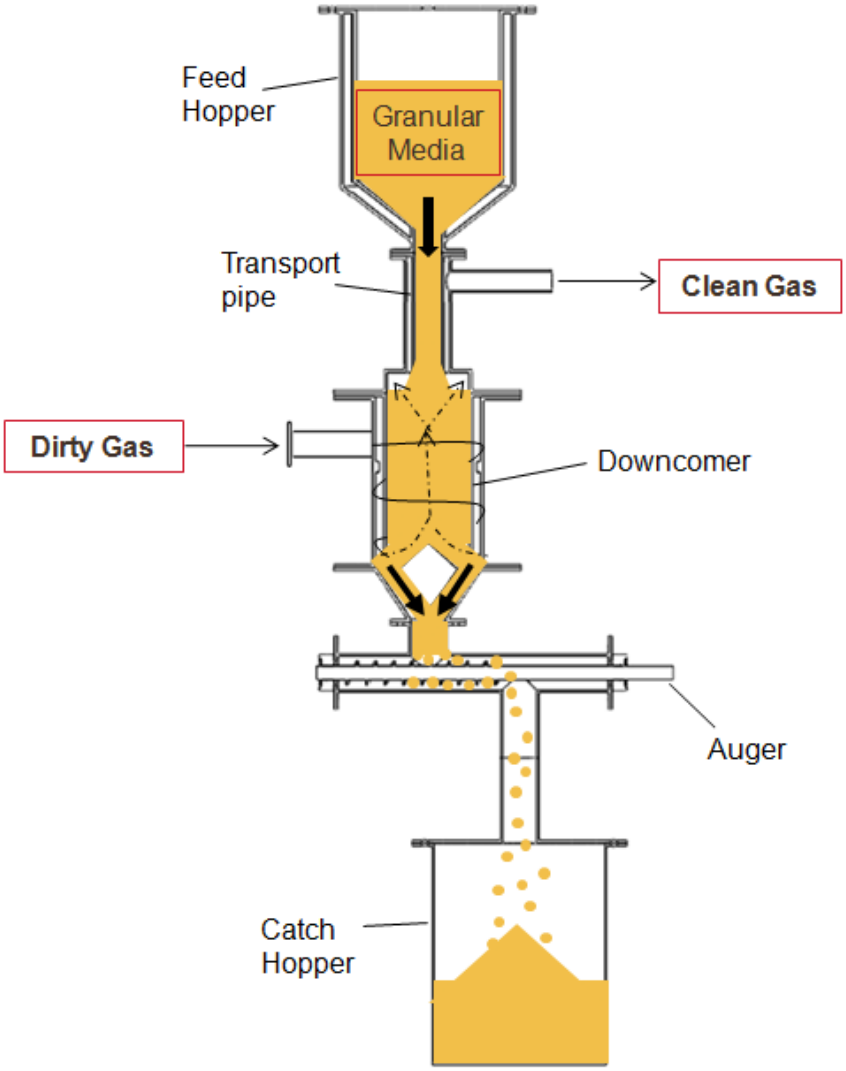

Figure 5: Schematic drawing of the MBGF

The aim of this work is to understand how granular flow rate affects the performance of the MBGF for the filtration of fast pyrolysis char. For this purpose, two variables are assessed; the collection efficiency, and dust accumulation within the filter's bed. Understanding how these variables are affected by the granular flow rate would help determine the operational criteria for high efficiency as well as the filtration capacity of the filter.

In order to determine the overall collection efficiency of the MBGF, a real-time process particle counter (PPC) is utilized. Moreover, several pressure probes are installed within and across the filter in order to assess the dust accumulation at the different bed regions. The following section 3.2 details the experimental setup and instrumentations used to achieve the experimental objectives.

3.2 Experimental equipment and setup

The research was performed on a 20 cm diameter moving bed granular filter, illustrated in **Figure 6** with dimensions.

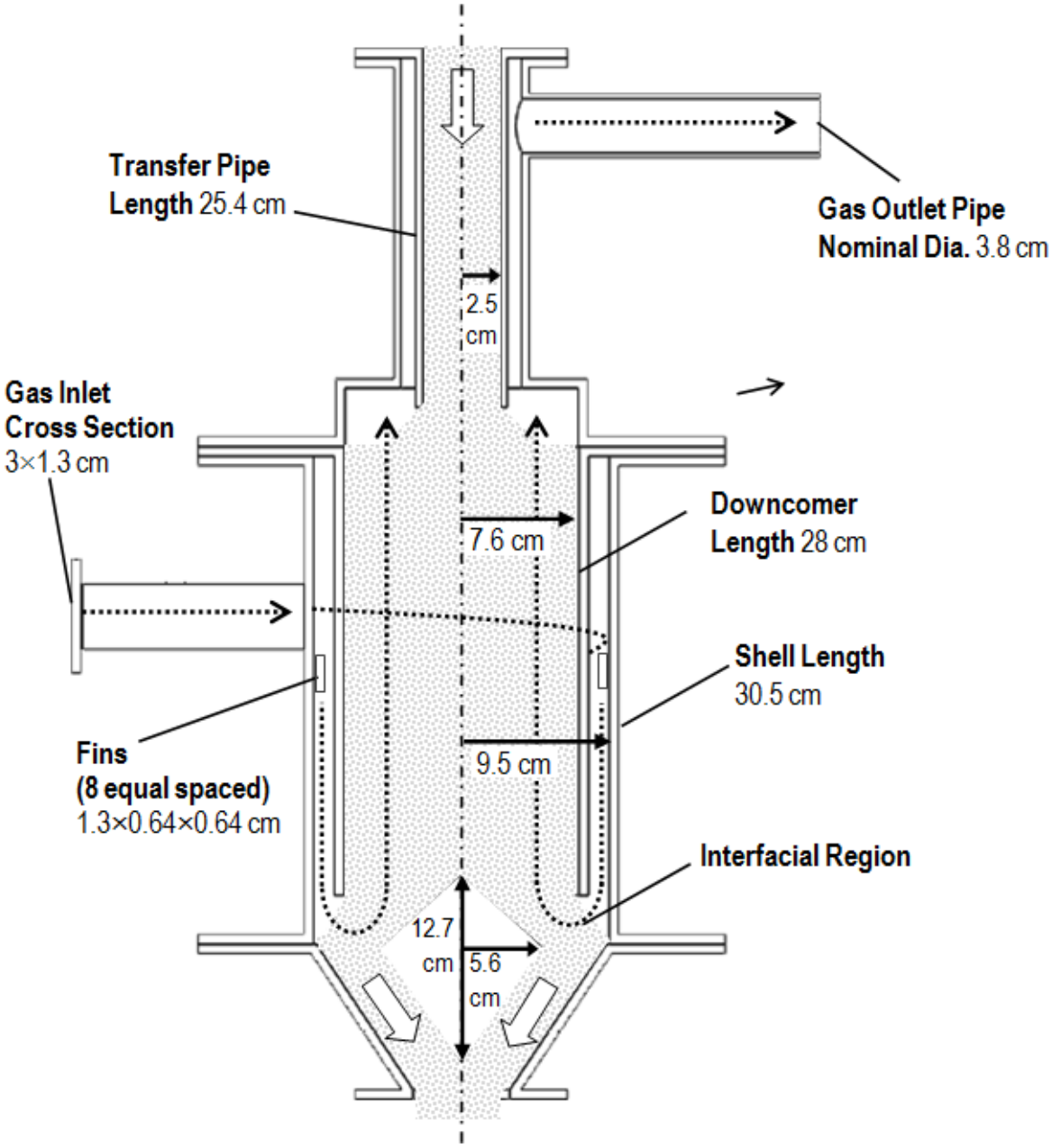

Figure 6: MBGF main body's dimensions

The air, typically at 600 slpm, enters the filter through a square tangential inlet which induces cyclonic flow. Fins are used to direct the flow horizontally downward before reaching the interfacial region where air first contacts the granular media. Eight fins are

equally spaced around the filter's shell in order to have uniform interaction with the entering gas right above.

The counter-current flow design collects high concentrations of dust at the interfacial region before reaching the filter's inner bed. This design allows the gas to flow through cleaner granules as it exits from the top of the downcomer. The granules enter the downcomer from a sealed storage vessel located above the filter. The flow rate of granules through the filter is controlled by an auger at the bottom of the filter. The dirty granules are augered into a sealed collection tank placed below the filter. A dividing cone is used to divert the granular forming the interfacial area. In order to eliminate static charge buildup the stainless steel shell and downcomer were grounded.

This study is performed at ambient conditions, as a precursor to hot filtration testing on the actual fast pyrolysis process development unit. In order to investigate the MBGF performance at ambient condition an experimental setup has been designed, which is shown in **Figure 7**.

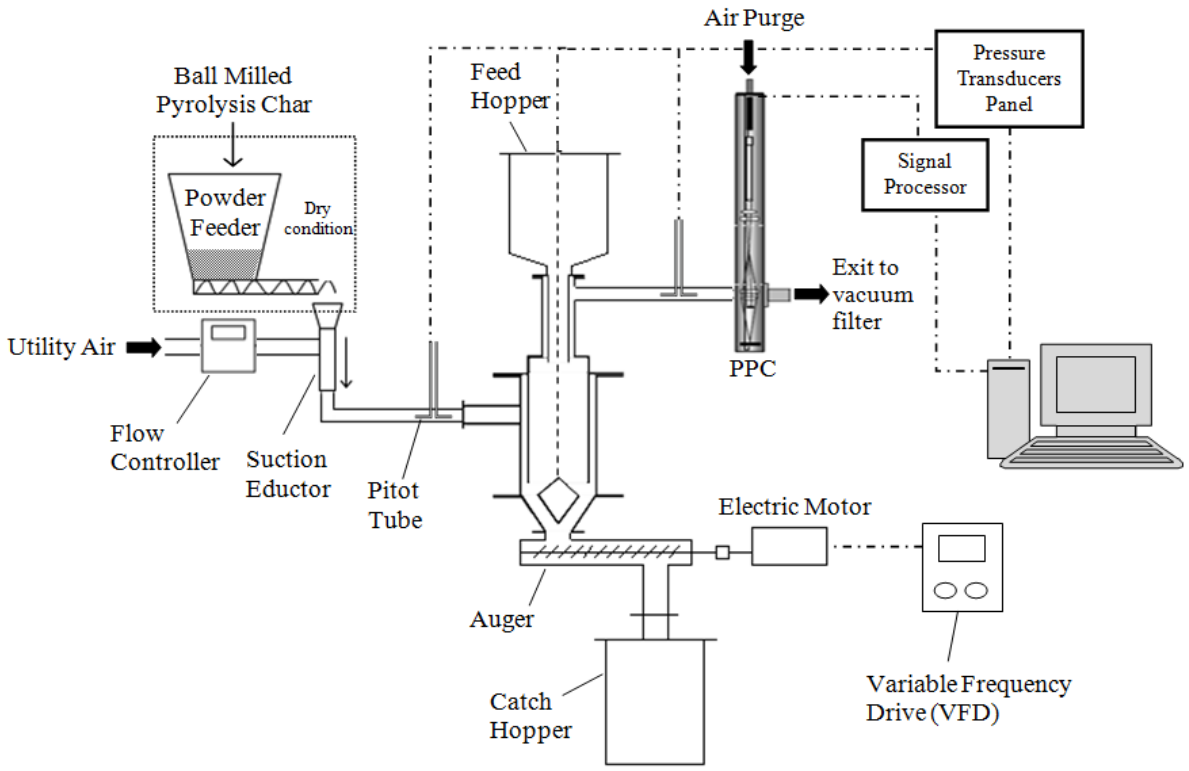

Figure 7: Experimental setup for cold flow testing

Air, utilized from a compressed air source, is controlled at the desired flow rate using Alicat Mass Flow Controller of 0-1000 slpm range. Pyrolysis char is ball milled to reduce its particle size before being fed through the calibrated powder feeder. A suction venturi eductor is used to entrain the char particulates into the main air flow. The suction force is created by passing the flow through two consecutive converging and diverging sections, where the suction is created in-between. The suction eductor was a crucial element in the char feeding, as it eliminated back pressure into the powder feeder that could result from increase in filter pressure. Moreover, it helps breakdown agglomerated char powder under the effect of shear force created by high velocity inside the venturi eductor while dispersing the powder into the gas stream.

Clean gravel granules of 2 mm average size are passed from the feed hopper through the main filter body. The flow of granules, granular rate (GR), is controlled by the auger rotation at the bottom of the main body. The auger is rotated using a three-phase electric motor which is controlled with a variable frequency drive (VFD). See **APPENDIX B** for the calibration curve of the VFD. The dust-laden granular media is augered into a sealed catch hopper at the bottom.

3.2.1 Pressure Instrumentation and Data Acquisition

Pressure measurement within the granular bed provides a tool to examine the regions where dust collections occur. When the dust laden gas pass through the filter bed it faces pressure drop due to contact with the granular media. Moreover, the collection of dust over the granules would decrease the volume void fraction in the bed, thus causing pressure drop to increase. In other words, pressure drop measurement would be a useful tool to assess the amount of dust accumulation on granules. In order to measure the pressure drop for several bed locations, five pressure taps (P0, P1, P2, P3 and P4) are inserted at 6.4 cm spacing along the axis of the bed, as shown in **Figure 8**. In this context the probes are termed *in-situ* pressure probes.

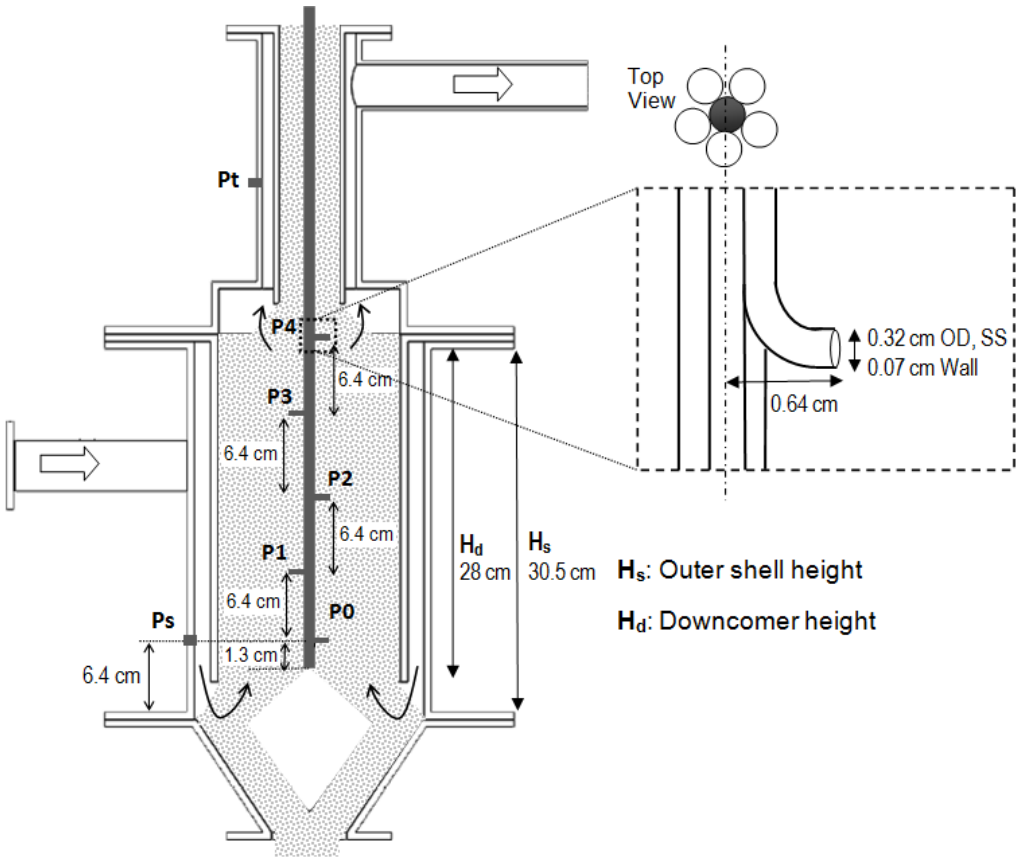

Figure 8: Schematic drawing of the in-situ pressure taps

Each of the in-situ probes is a 0.32 cm outer diameter stainless steel tube. All the in-situ probes are bundled on a central tube held between the cone's top and the feed hopper. The tubes are passed through the transport tube to the top of the feed hopper where they are connected to their respective pressure transducer. The pressure taps are designed to measure the static pressure; hence they are set to be perpendicular to the flow. Even if dynamic pressure is measured by the pressure taps, it would induce an error than 0.02% error in pressure measurement. **Table 1** shows the calculation of dynamic pressure and potential error in measured pressure.

Table 1: Comparison between the dynamic and measured pressure in the downcomer

Air flow rate (Q)	Downcomer superficial velocity, (U_d)	Dynamic pressure, calculated ($\frac{1}{2} \times \rho \times U_d^2$)	Measured pressure	Possible error
650 l/min	0.594 m/s	< 0.001 in-H_2O	5-20 in-H_2O	< 0.02%

The differential pressure between the pressure tap (Ps) located at the outer shell and the pressure tab (Pt) located before the outlet pipe is used to identify the pressure drop of the granular bed (ΔP_{bed}), encompassing both the interfacial region and downcomer region. The pressure drop between Ps and the lowest in-situ pressure tap in the downcomer (P0) is used to identify the pressure drop as the interface ($\Delta P_{interface}$). For simplicity of analysis, the downcomer region, between P0 and P4, is divided into two regions R1 and R2, see **Figure 9**. The pressure drop terms and descriptions are listed in **Table 2**.

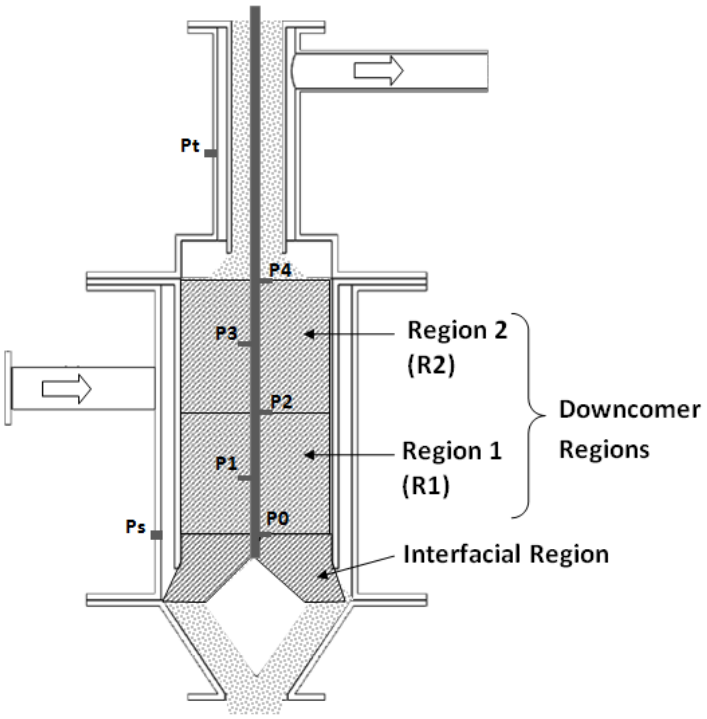

Figure 9: MBGF's regions

Table 2: Pressure drop measurements inside the MBGF

Pressure Drop Region	Term	Tap differential
Granular Bed	ΔP_{bed}	$Ps - Pt$
Interface	ΔP(interface)	$Ps - P0$
Downcomer, Region 1	ΔP(R1)	$P0 - P2$
Downcomer, Region 2	ΔP(R2)	$P2 - P4$
Downcomer, Region 1 & 2	ΔP(downcomer)	$P0 - P4$

In order to check the probes accuracy with respect to their location, the pressure readings at different air flow rates are compared with the pressure drop obtained from theoretical equations for packed beds. Ergun equation is used as a correlation to obtain the pressure drop along the length of a packed bed for the flow of fluids. A modified version of Ergun equation, known as McDonald equation, has better agreements with experimental air flows results. The experimental pressure measurements are in good fit with the predictions of

the McDonald equation [18]. See **APPENDIX A** for the comparison between the experimental fixed bed pressure measurements compared to the theoretical predictions.

The pressure transducers utilized are Dwyer 677 Differential Pressure Transducers. **Table 3** shows the measurement range and accuracy of each transducer. The transducers are connected to a National Instruments SCXI-1000 chassis which transmits the data readings to LabVIEW 8.2 software. In this method, the signals from the pressure transducers can be collected and recorded. Transducer calibrations are stored in the software to convert the electric signal data into pressure data. The software reads the electric signal data at 100 Hz and records the averaged data at a desired 1 Hz sample rate. The data is then saved and analyzed in a spreadsheet file.

Table 3: Measurement range of Dwyer 677 differential pressure transducers

Probe Location	Measurement Range and Accuracy
Ps, P0, P1	0-25 inches H_2O at 20°C, ±0.1
P2, P3, P4, Pt	0-15 inches H_2O at 20°C, ±0.06

3.2.2 Process Particle Counter (PPC)

A process particle counter (PPC) device manufactured by Process Metrix is used to determine the filter's outlet flow particulate measurement. The PPC utilizes dual laser beams to count the number and size of the particulates passing through the gas stream. This device can measure particulate concentrations of less than 10^7 particle/cm^3 [28], which lies within the expected outlet concentration.

The PPC is designed to operate at high temperature and pressure, up to 1370 °C and 80 bar. It is equipped with circulating cooling system to prevent the instrument overheating. Since the experiments performed in this study are at ambient conditions, the cooling system was not used.

The PPC measures particulates using the laser light scattering principle [28], see **Figure 10**. The PPC has two monochromatic laser beams, each designed to measure a certain particle size range. The larger beam, having a wavelength of 150 nm, is capable of measuring particles in the range of 3 – 80 µm, while the smaller beam of 30 nm wavelength can measure particles in the range of 0.3 – 2 µm. The two beams works in succession alternating every few seconds. Since larger particles account for larger mass, more sampling time is needed using the large beam to minimize errors in calculating the mass concentration. In this study 70% of the total measurement time is specified for the larger beam and 30% for the smaller beam. The total time of the two beams working is called the update period. An update period of five seconds is selected in this study as a relatively optimum sampling time.

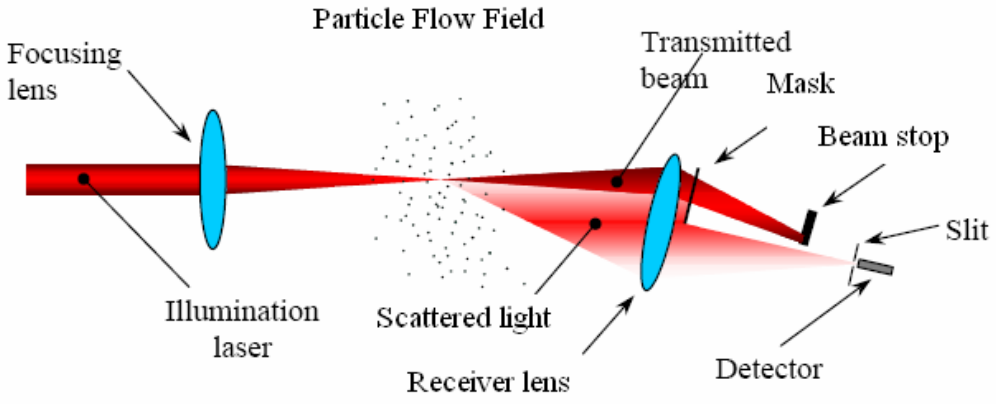

Figure 10: Basic operating principle of the PPC [28]

The emitted light is scattered when it impacts a particle; with several particles flowing in the stream the light scatters in different directions. The scattered light is directed using a converging lens to a photomultiplier detector. The detector reads the light intensity and converts it into voltage amplitude, which is proportional to the particle diameter. The width of the voltage signal is proportional to the particle's velocity. The rate at which scattering occurs corresponds to the particle count. Using the particle count and diameter and velocity the mass concentration could be calculated.

The photomultiplier is set to a voltage level where successive voltage peaks could be read above this value, such value is called the discriminator level. When relatively high concentration of particles exists in the flow, the voltage signals could overlap causing the signal processor to analyze these signals as one large signal. Such overlap causes an overestimate of actual concentration. In order to avoid this, the discriminator level has to be raised; however this would lead to skip detecting smaller peaks. **Figure 11** shows how signal overlap might occur and the appropriate discriminator needed.

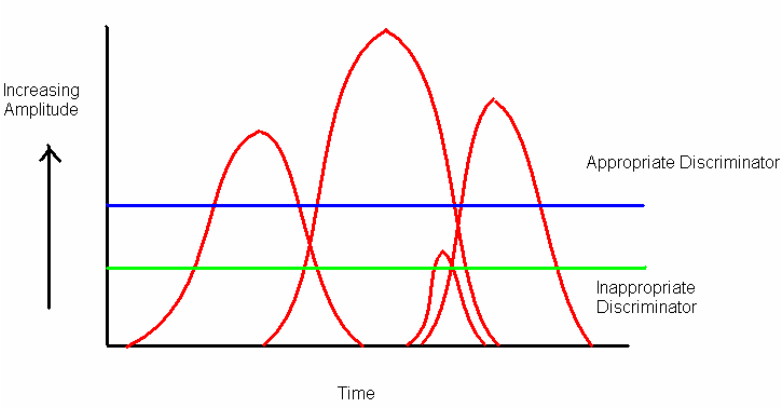

Figure 11: Signal overlap and required discriminator level [10]

The PPC is in the shape of long tube which is mounted perpendicular to the flow. **Figure 12** shows detailed drawing of the PPC and its inside schematic. The main gas stream is passed through a rectangular shaped flow section within the PPC. The laser beams traverse between the two far sides of the rectangular cross section. Glass window on both sides transmit the laser beam to the flow. In order to keep the windows clean of dust, purge air is supplied on the surface of the windows.

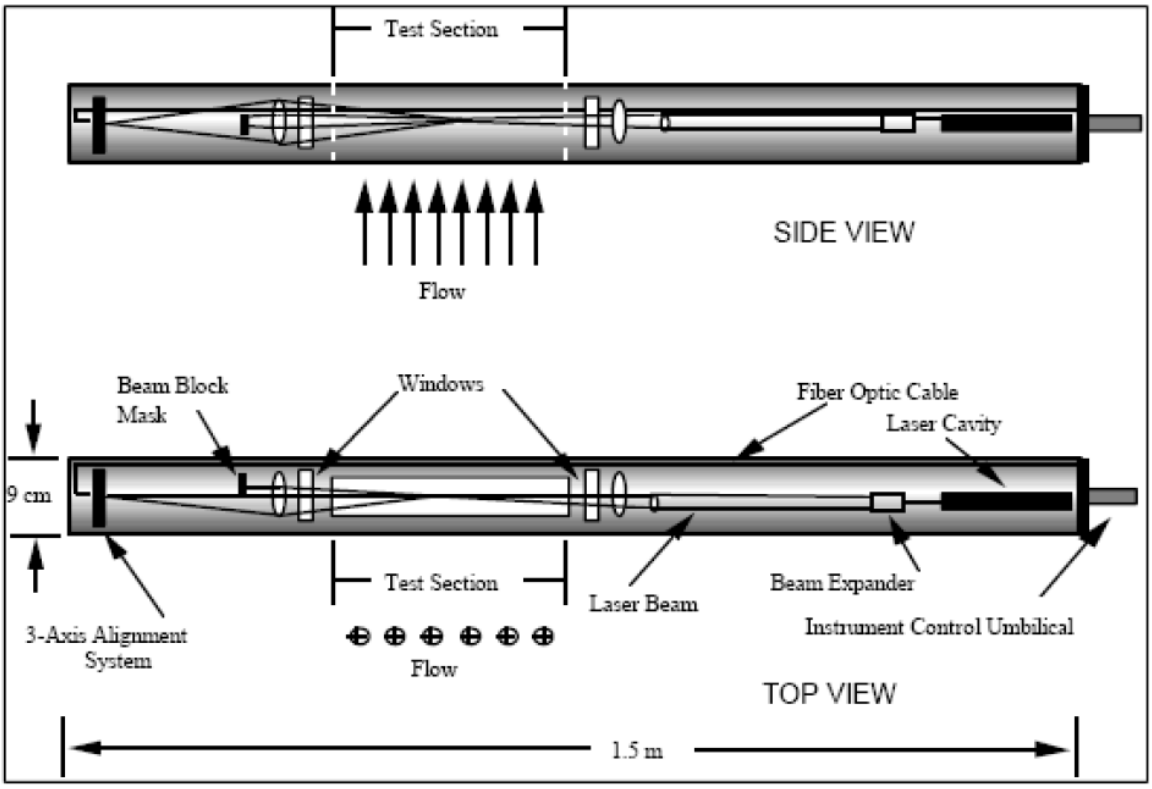

Figure 12: PPC's top and side view and its inside working schematic [28]

The PPC is calibrated by collecting the gas-laden dust using a bag-house filter installed after the PPC. The amount of dust which passes through the PPC is identified by measuring the difference in mass of the bag filter before and after the calibration time. The

amount of collected dust is compared to the time integration of the PPC's instantaneous mass concentration measurement. The PPC was found to be consistent up to 95% accuracy.

3.2.3 Powder feeding and calibration

Char powder feeding and dispersing into a gas flow is a very challenging task. Firstly a powder feeder made by Powder feed Dynamics (Mark XV) was selected for char feeding and dispersion. The powder feeder has a pressurized powder canister where char is withdrawn at the bottom using a 0.64 cm motor-driven auger into a carrier stream, which then joins the main air stream to the filter. The canister is agitated using a vibrating motor to compact the powder on the feeding auger. However, several problems were faced using the pressurized system. Due to the char's low density, the pressure caused the char to fluidize resulting in an inconsistent feeding. Moreover, it is difficult to accurately calibrate the filter using such a setup, since it becomes a challenge to catch and measure the gas entrained dust after leaving the feeder. To overcome these challenges, the system was modified by removing the pressure and the gas carrier stream. The char would be then fed using the metering auger which delivers the powder to fall on top of a venturi suction eductor installed on the main air stream.

Moreover, it was observed that high air humidity was causing the char to absorb air moisture and agglomerate. For this reason, an air conditioned enclosure was built for the powder feeding system, where dry air exiting the air conditioner would replace the humid air around the powder feeder, as shown in **Figure 13** below.

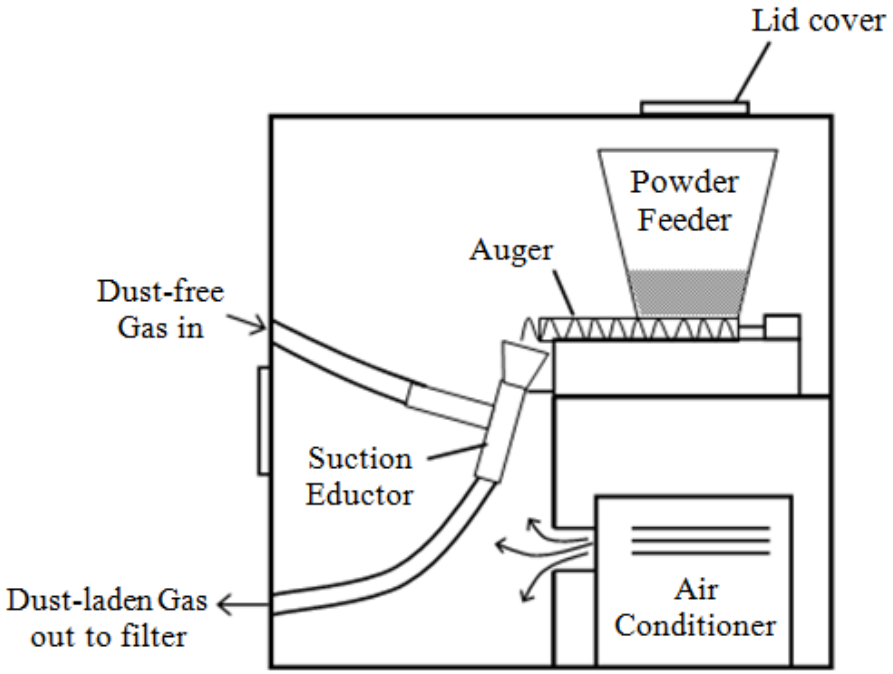

Figure 13: The enclosed and air conditioned powder feeding setup

The powder feeder is calibrated by placing a pre-weighed collecting cup at the feeding end of the auger. The powder feeder is set to vibrate, causing the char to compact over the auger, and the auger is set to rotate at a desired rotation per minute (RPM). Calibration is performed over a feeding time, from 5 - 30 minutes, and then the cup is weighed. The mass of the collected char (g) is divided over calibration time (min) to find char feed rate (g/min).

In order to attain near accurate feeding during the experiment, the powder level in the feeder is maintained at a marked level. This is achieved by adding char each 20 minutes of powder feeding. The amount of char added corresponds to that amount fed over the 20 minute period. The added char amount should bring the char level in the hopper back to its

initial height. The feeder's hopper is color marked at several height levels, thus char level could be observed.

3.3 Materials

3.3.1 Granular media

The granular material used in this research is water filtration gravel obtained from Red Flint LLC. The gravel obtained has a rectangular equivalent size of 3.2 mm by 1.6 mm, which is the smallest size in the gravel classification. This granular size has been selected since previous researchers [9, 10] obtained high filtration efficiency for this size.

The purchased gravel contains significant amount of dust which elutriates with air when placed in the MBGF. This would create an error in measuring the actual penetrating char particle by the PPC. In order to eliminate the gravel dust, a cleaning method was devised using the MBGF itself. The MBGF is filled with the originally received gravel through the feed hopper. The flow through the filter is set at 900 SLPM, which is enough to elutriate the dust particles that are below 500 μm and flow through the filter's exit. At the same time the gravel is augered at a fast rate of 40 kg/hr, which makes the process quick and continuous. The cleaned gravel is collected in the catch hopper and is then used for the filtration test.

3.3.2 Char preparation

The char used in this study is obtained from a fast pyrolysis process development unit (PDU) built and operated at the Iowa Energy Center's Biomass Energy Conversion Facility (BECON). The PDU process utilizes fluidized bed as a reactor followed by two successive

cyclones for char separation [29]. The collected char from the cyclone catches has a wide particle size range from 5 – 600 μm. The collection efficiency of the cyclones is less for the small particles which are under 50 μm [30]. In order to mimic the particle size range that is exiting the cyclones, the collected char needs to be reduced in size. Since it was not feasible to measure the particle size distribution for the cyclones' exiting stream, the objective is set to reduce the collected char size as much below 50 μm.

The collected char is first sifted using a mechanical sieve shaker. Particles that falls below the 300 μm standard mesh size are taken for ball milling for further size reduction. The char is placed in the ball mill inside a ceramic cup containing 5 mm ceramic balls. The cup is sealed and spun around using an electric motor. The centrifugal force causes the balls to rotate inside the container and grind the char. The ball milling is optimized to run for 20 minutes to produce particles that have 20-25 μm volumetric average mean. The size reduction procedure is performed in a dry air conditioned room to eliminate humidity.

In order to measure the resulting char size distribution, a Malvern particle sizer 2000MU is used. The sizer utilizes the coulter principle of particle counting, and has a wide measuring capability for particle size range 0.02-1000 μm. A small amount of char, around 0.5 g, is mixed with 600 ml de-ionized water in a 100 ml beaker. An ultrasonic vibrator that is installed with the Malvern equipment is used to breakdown any char agglomeration in the de-ionized water. Then water is circulated through a windowed cell where the laser passes. Similar to the diffraction principal used in the PPC, the laser diffraction determines the particle sizes. **Figure 14** shows the char size distribution after size reduction procedure.

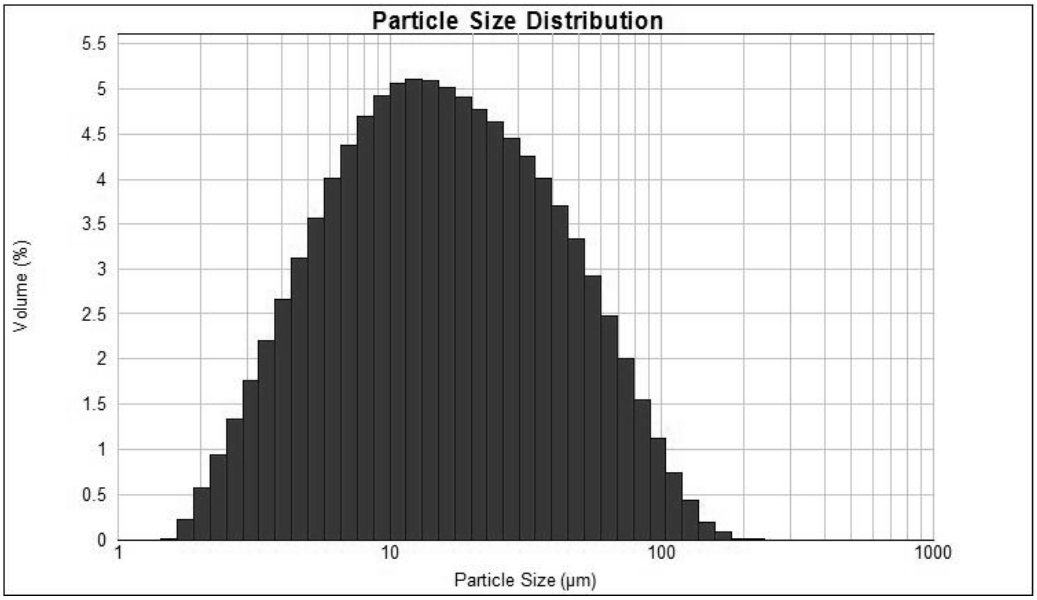

Figure 14: Particle size distribution by volume of the size reduced char

In this research, the char is obtained through pyrolyzing switchgrass, as the biomass feedstock, using the PDU. **Figure 14** shows the particle size distribution of the reduced size char, which yields a volumetric weighted mean particle size of 24 ± 1 µm, and 90%, undersize diameter of 56 µm.

3.3 Experimental Procedure

Running a relatively large system with many instrumentations and variables requires careful check before running any experiment. To begin with, before each test the powder feeder must be calibrated, using the calibration method described earlier, for a minimum of one hour calibration time. The calibrated data is used to calculate the inlet char concentration of that test.

Before using the PPC, its windows are cleaned before each test. Then the PPC is mounted at the exit of the MBGF and connected with the signal processor. An air purge stream is connected to the PPC to keep the PPC windows clean of dust. The PPC software and the LabVIEW control software is turned on at this time. The purge flow through the PPC is then set at a flow rate value between 100 to 150 SLPM. Turning on the PPC's signal processor connects the PPC with its software. The PPC is controlled using the software, so once all the cables are well connected, the software shows the processor and the PPC are connected and indicate their internal temperatures. The laser measurement is started by clicking the start button on the PPC's software. The power of each laser beam is displayed in the software while running. The power value for each beam should be the same value before every test. If the power is significantly less, its means that the windows have dust on them and need to be cleaned. While there is no air passing through the MBGF, the PPC displays pink records, which means no particles are detected.

The MBGF is filled with the cleaned gravel from the feed hopper. The feed hopper can hold around 40 kg of the 2 mm gravel, while the filter main body can hold around 8 kg. The feed hopper is then sealed and the main air flow is started by setting the desired control value in the LabVIEW program, e.g. 600 SLPM. All joints and flanges are then checked for leakage using soap solution. At this time, the LabVIEW program shows the pressure measurements across the filter and within the bed.

After initial filling of the MBGF with gravel, the granular withdrawal is started. The filter's pressure drop decreases over time until it reaches steady state. In order to reach steady state faster the granular material is withdrawn at a faster speed. The withdrawal is run until

the filter's bed gravel is replaced by new gravel twice. After that, the auger is set to rotate at the desired rotational speed for the filtration test.

The char feeding is then started, and starting time is recorded. During the feeding time, char is added to the powder feeder every 20 minutes in the amount equivalent to 20 minutes of feeding. This is required to keep the powder feeder running at steady conditions.

To terminate the test, the powder feeder is stopped and main airflow is shutdown. The remaining gravel inside the filter is withdrawn completely from the filter and the filter is cleaned by flushing the filter with air at 1000 SLPM for 30 minutes, to be ready for another test.

CHAPTER 4. RESULTS AND DISCUSSION

4.1 Experimental Design

Experiments were designed to identify the effect of granular flow rate on char accumulation and collection efficiency over time. Two main hypotheses are to be tested; the first is that dust collection occurs mostly at the interfacial region, as observed by previous researchers. The second hypothesis is that the moving bed filter needs to be operated above a minimum granular withdrawal rate to prevent excessive dust loading in the bed, which degrades filtration efficiency. **Table 4** below lists the moving bed filtration experiments to be performed at different granular flow rates.

Table 4: Experimental variables

Air Flow Rate (Q) - slpm	**Char Feed Rate (Mc) - kg/hr**	**Granular Flow Rate (Mg) - kg/hr**	**Mgravel/Mchar** $\frac{Mg}{Mc} \equiv \frac{[kg/hr]}{[kg/hr]}$	**Granular Residence Time (t_g) - hr**
620	0.103	3.3	**32.0**	**2.44**
		5.3	**51.5**	**1.51**
		7.3	**71.0**	**1.10**
		9.3	**90.5**	**0.86**

The granular residence time (t_g) is calculated by dividing the mass of the bed over the granular flow rate:

$$t_g = \frac{Mbed}{Mg} = \frac{8kg}{Mg(kg/hr)} \qquad \text{Equation (8)}$$

The fast pyrolysis development unit at BECON could utilize around 8 kg/hr of biomass. The fast pyrolysis produces between 10-15%wt char. Assuming that the cyclones collects 90% of the char, the amount of char to be filtered by the MBGF is around 0.1 kg/hr. The 620 slpm of air is selected as a median flow rate similar to previous researcher [9, 10]. The equipment was designed to operate around such flow rate, which is enough not to cause fluidization of the granular media.

4.2 Effect of granular flow rate on collection efficiency

The PPC instrument monitors the concentration of char exiting the filter in real-time, which allows the instant measurement of collection efficiency of the moving bed filter. The results of moving bed filtration experiments over time are shown in **Figure 15**. The time is reported in a dimensionless term (τ), which is the experiment time (t) divided by the granular residence time t_g of that experiment:

$$\tau = \frac{t}{t_g} \qquad \text{Equation (9)}$$

Experiments are run up to a τ of 1.5, in order to permit the granular media in the filter bed to entirely refresh. A series of three test trials was conducted for each granular residence time (t_g) variable. The error intervals are 95% confidence intervals; see **APPENDIX C** for the total uncertainty calculations.

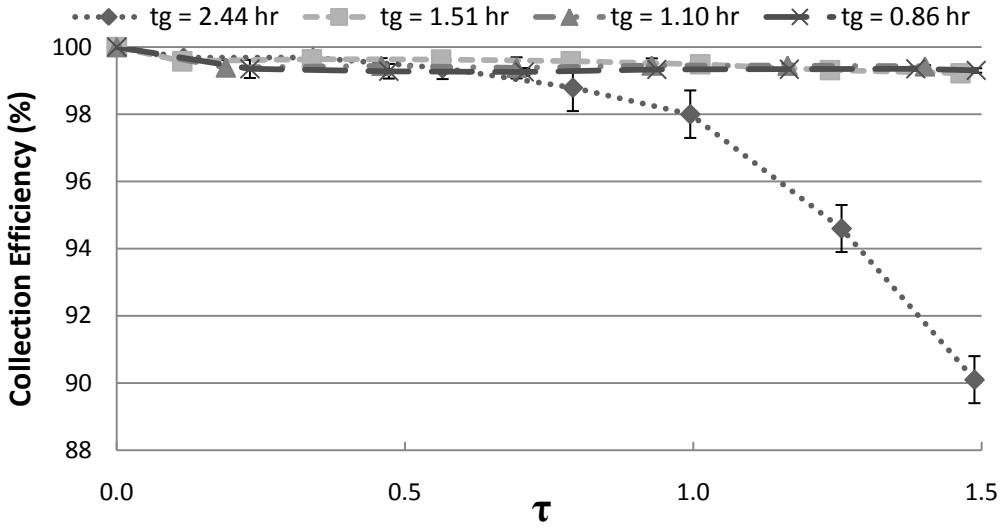

Figure 15: Collection efficiencies of MBGF experiments

The results shows that the collection efficiency decreases significantly for the experiment with the highest granular residence time (t_g=2.44 hr), whereas the other residence time experiments exhibit steady state high efficiency collection (>99%). This suggests that the MBGF has to be operated lower than a critical t_g to maintain steady state in efficiency. A closer look at high efficiency range (98%-100%), as shown in **Figure 16**, shows that the results of experiments of t_g 0.86-1.51 hr are in close proximity of each other. In fact, ANOVA statistical comparison between the experiments for t_g 0.86-1.51 gives a P-value >0.05 for all the result points, indicating there is no significant statistical difference among them.

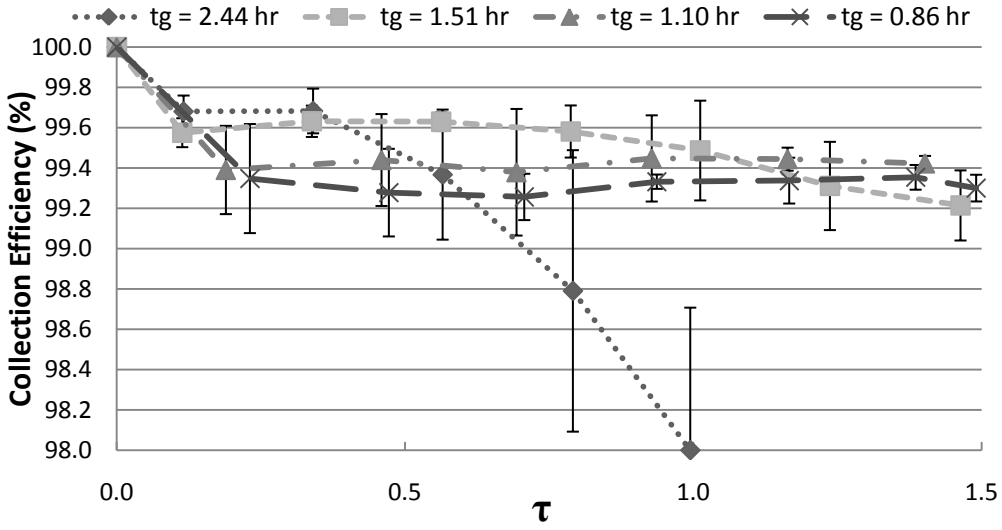

Figure 16: Collection efficiencies of MBGF experiments, zoom-in view of Figure 15

The results could explain the reason why some literature indicated that increasing granular flow rate has no significant effect on efficiency [24], while others reported it had an improving effect [8]. The conclusion is verily dependent on the investigated range of granular withdrawal rate and dust inlet concentration, as well as the length of experiment. For example, if the experiment of t_g=2.44 hr was stopped when τ=0.5, the conclusion would be statistical insignificant from lower residence time experiments.

4.3 Pressure drop vs. char accumulation

The filter consists of two distinct filtration sections; the interfacial region and the downcomer region. It is difficult to exactly measure the efficiency of each section, however, it hypothesized that pressure drop for the granular bed, which is easily measured, correlates with the amount of dust captured. The efficiency of the sections could be calculated from the dust accumulation data, as subsequently documented.

In order to obtain the correlation between increase in pressure drop and amount of char accumulation, the filter is disassembled after each moving bed filtration test and gravel from each region is weighed then sifted to separate it from the collected char. The loss in weight of the sifted gravel corresponds to the amount of collected char. The respective increase in pressure drop is the difference between the pressure drop value at the end of the test and its start. Pressure drop is represented in a dimensionless term $\frac{\Delta Pc}{\frac{1}{2}\rho V^2}$, where ρ is the gas density, V is the gas superficial velocity, and ΔPc is the corrected pressure drop which is the difference between the measured pressure drop and the pressure drop when the bed contains no dust. The dimensionless pressure term represents the ratio of static pressure over dynamic pressure. **Figure 17** shows the obtained correlations for the whole filter bed, interfacial region and Region 1. Char accumulation in Region 2 was insignificant and is not calculated in this figure.

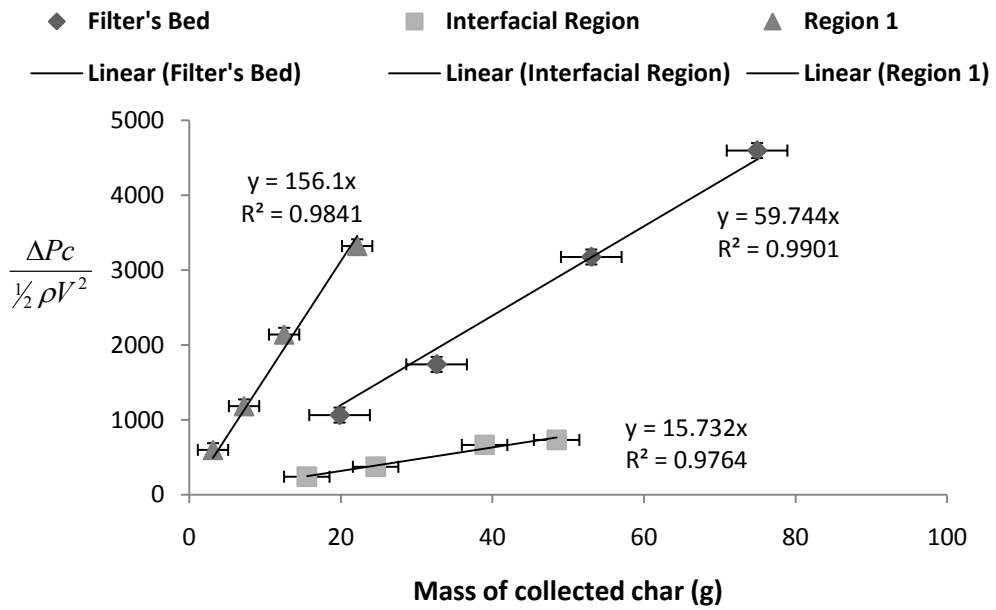

Figure 17: Pressure drop vs. accumulated char for the bed, interface & R1 regions

The results indicate there is a linear relationship between the pressure drop and char accumulation. Char accumulation decreases bed void which causes the air to flow through smaller spaces which increases pressure drop. Char accumulation can be correlated in McDonald's pressure drop equation as decrease in void fraction (ε) or increase in particle diameter (Dp), See **APPENDIX A** for McDonald's equation expression. The change in either terms leads to an exponential-like increase in pressure drop. **Figure 18** shows how the pressure drop would change due to decrease in bed void as predicted by McDonald's pressure drop correlation.

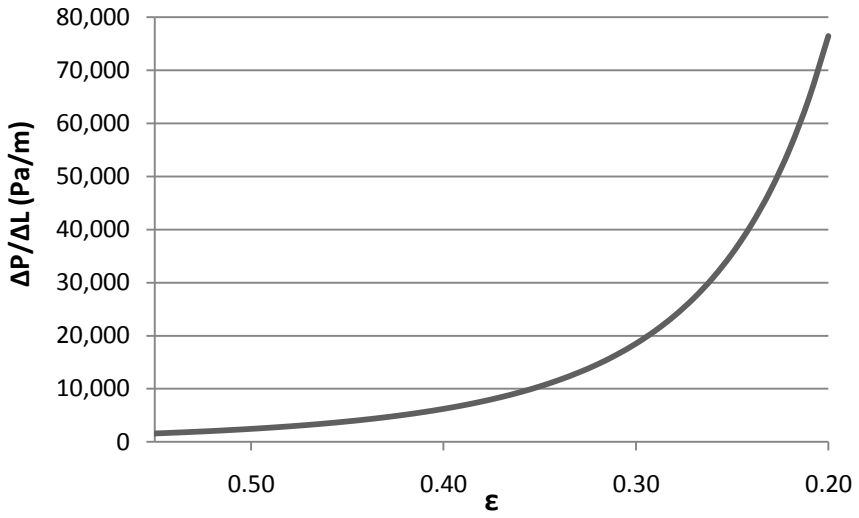

Figure 18: Pressure drop vs. bed void, McDonald's equation

The appearance of linear relationship in pressure drop suggests that voidage only increases a small amount during filtration. For instance, the estimation for decrease of voidage for an accumulation of 20 g of char particles in an inch of height in region 1 is approximately 0.043. While an accumulation of 50 g in the interfacial region would result in

an estimated 0.054 decrease in voidage. Calculations are shown in **APPENDIX D**. As seen in the previous figure, a bed void change of less than 0.1 would look less exponential.

Moreover, the results show that the slope of pressure drop increase in Region 1 is higher than that at the interfacial region. That is, the interfacial region can hold more char per unit increase in pressure drop than region 1. The difference between the regions is due to the fact that the interfacial region has larger initial void fraction than region 1.

When filling the MBGF with the granular material, the particle settles randomly and compact creating a certain void fraction. Once the granular withdrawal from the bottom is started, the granules tend to space out and move downward, which is evidenced by the decrease in pressure drop across the bed and its regions, as shown in **Table 5**.

Table 5: Pressure drops (in-H_2O 20ºC) for moving bed before dust accumulation

	ΔP bed	**ΔP (interface)**	**ΔP (R1)**	**ΔP (R2)**
Fixed Bed	10.8	2.9	3.9	3.3
Moving Bed	7.9	1.1	3.3	2.8
Difference	2.9	1.8 (62.1%)	0.6 (15.4%)	0.5 (15.2%)

The downcomer regions, R1 & R2, exhibit moderate decrease in pressure drop, however the interfacial regions shows the highest decrease in pressure drop, i.e. more than 60% of its initial value, indicating that the interfacial region has a much larger void fraction. This could be attributed to the geometrical shape of the interfacial area. Underneath the downcomer's edge the granules face a sudden increase in cross sectional area, forming the

inclined interfacial surface. This would result in a larger spacing between the granules with less hydrostatic pressure from the downcomer's section.

The obtained pressure drop correlations are used in the next section for estimating the accumulation of char over time in the filter's whole bed and regions.

4.4 Effect of granular flow rate on char accumulation

During each experiment, the instantaneous pressure drop is measured. Using the correlations developed in section 4.3, the amount of char accumulation over time is estimated. **Figure 19** shows the resulting char accumulation inside the MBGF for the granular flow rates experiments.

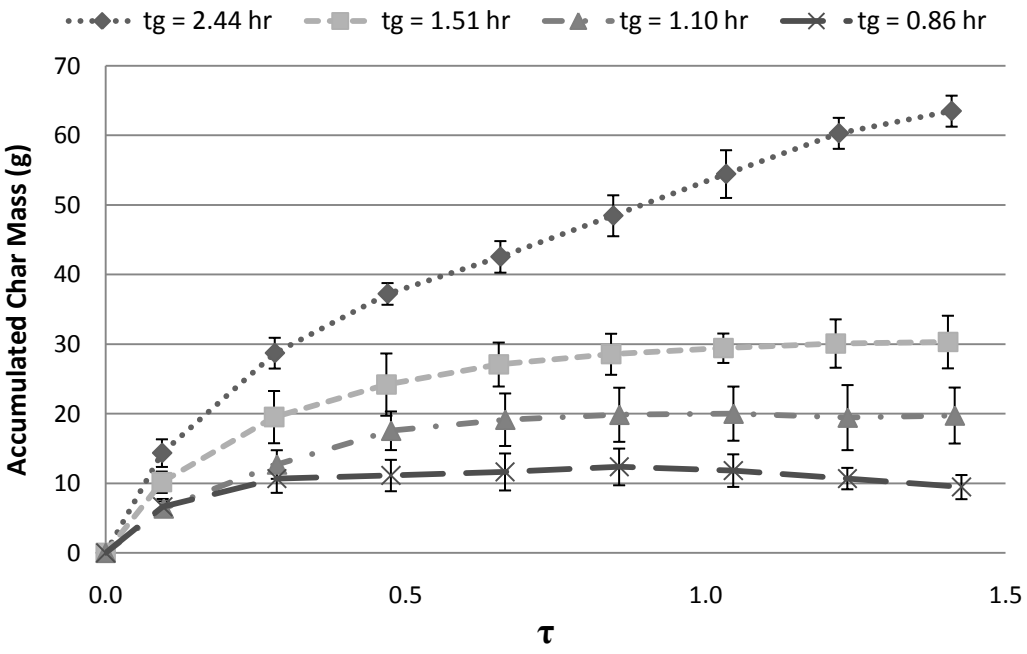

Figure 19: Char accumulation inside the MBGF as a function of dimensionless time

The char accumulation over time shows a close approach to steady state for experiments of t_g 0.86-1.51 hr. Steady state occur when dust is removed from the gas flow at the same rate dust is withdrawn from the bed. Reaching steady accumulation indicates that the filter is collecting char as much as it is withdrawing out of the filter. Moreover, as the granular residence time t_g is decreased, there less char accumulation, since the collected char is withdrawn at a faster rate out of the filter.

At τ=1.0 the MBGF should reach 63% of the steady state value in plug flow, see **APPENDIX E** for derivation. While this is occurring for all cases except for experiment with the longest residence time of t_g=2.44 hr. In this case char accumulation continues to increase over the investigated time, which indicates that the withdrawal rate of collected char is slower than the char collection rate. The filter could be said to "clog" with char, and promote re-entrainment of char which penetrates the filter, as it shows in efficiency decrease in **Figure 15**. In order to understand the reasons for such phenomena, the char accumulation in each bed region is examined in **Figure 20**.

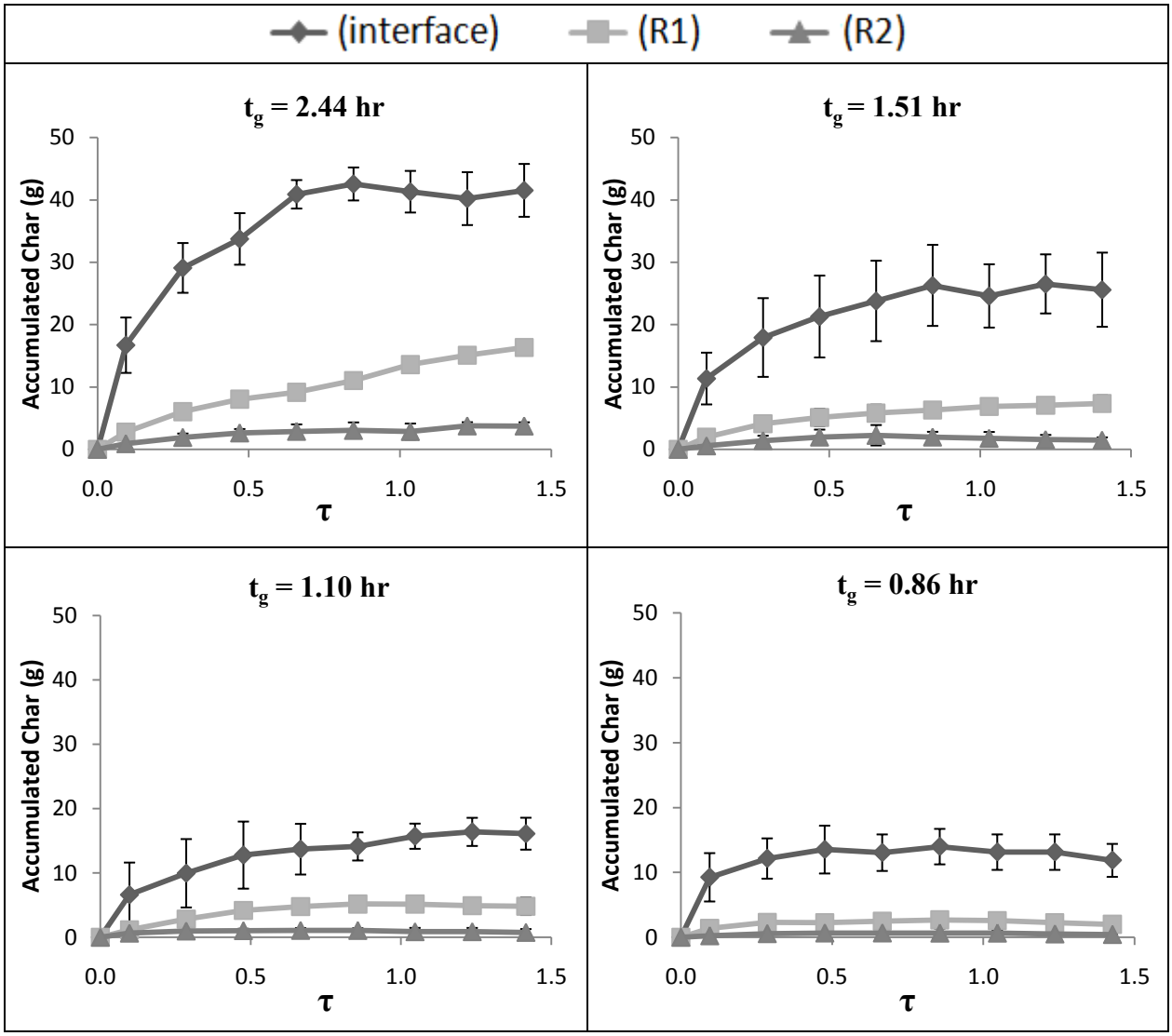

Figure 20: Moving bed filtration; bed regions' char accumulation

Similar to the bed's char accumulation, the char accumulation of the bed regions approaches steady state for experiments of t_g= 0.86-1.51 hr. The experiment at t_g= 2.44 hr shows that the interfacial region reaches a steady value, whereas region 1 and 2 continues to accumulate more over time. This indicates that the granular withdrawal is not fast enough to keep the downcomer regions from continuously accumulating.

Figure 21 below shows how region 1 and 2 plays an increasing filtration role as t_g increases. The accumulation profile across the filter's height looks much like an absorption filter, until eventually at the highest t_g becomes overloaded with dust causing breakthrough.

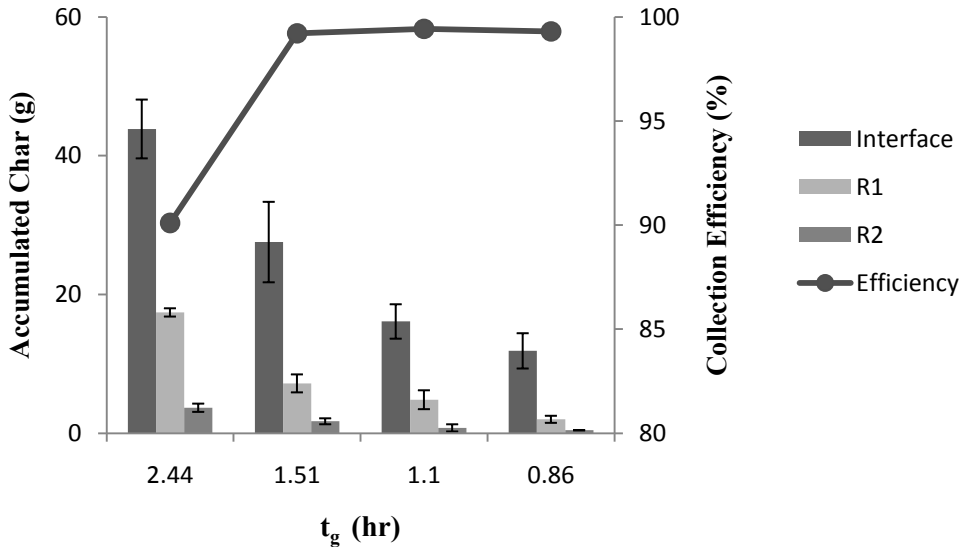

Figure 21: Accumulated char for bed regions and filter's efficiency at τ=1.5 as a function of granular residence time

Inertial impaction is the dominant filtration mechanism in granular filtration [18], and is characterized by the Stokes number. **Table 6** below shows the Stokes numbers associated with the char in this research. The numbers are based on the average geometrical particle size determined from the particle size distribution. See **Appendix G** for the calculation of the Stokes numbers.

Table 6: Stokes numbers

	Interfacial Region	**Downcomer Region**
Stokes number (St) 24 μm	2.486	0.967

The interfacial region has a larger Stokes number than the downcomer region due to the higher superficial velocity at the interface. Particles with Stokes number less than unity are more likely to follow the gas stream lines without impacting on the granular surface [18]. This would explain the reason why char accumulates less significantly in the downcomer regions. Another reason for the high efficiency of the interfacial region, is the formation of a dust cake layer which is said to improve collection efficiency [6, 11] by inducing straining effect.

Performing mass balance around the interfacial and downcomer regions, as shown in **APPENDIX F**, permits us to examine the collection efficiency of each region. **Figure 22** shows the collection efficiency for the interfacial and downcomer regions of the moving bed experiments.

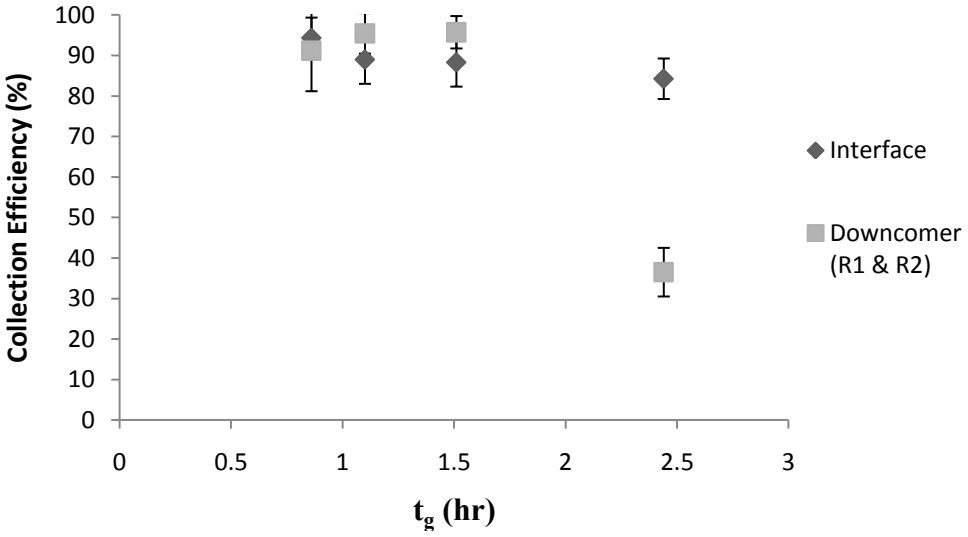

Figure 22: Collection efficiency of bed regions at τ=1.5

As the efficiency results show, at t_g= 2.44 hr the downcomer region becomes less efficient due to the high granular residence rate and higher influx of dust from the interfacial region. Hence, it is critical to maintain most of the dust collection at the interfacial region with sufficient granular flow rate.

4.5 Granular flow rate operation criteria for high efficiency

Section 4.2 revealed that granular residence time has to be low enough to maintain high efficiency. In the previous section 4.4, it was identified that the downcomer region is less efficient than the interfacial region due to lower Stokes number. Thus, the criterion to maintain high overall efficiency is to decrease the char penetration to the downcomer region. In order to indentify such criterion, a dust volumetric fraction (υ_d) variable is defined, which is the ratio of dust volume over the volume of dust and granules.

$$\upsilon_d = \frac{V_d}{V_d + V_G} = \frac{1}{1 + \frac{\rho_{bd}}{\rho_{bG}}\left(\frac{M_G}{M_d}\right)}$$ Equation (10)

Where M_G and M_d are the mass of granules and char dust, while ρ_{bd} and ρ_{bG} are the bulk densities of dust and granules, respectively. The critical dust volume fraction (υ_d*) is defined as volume fraction reached when efficiency starts to drop. That is when the filter starts to "clog". **Figure 23** shows the dust volumetric fraction in interfacial and R1 regions reached for the moving bed experiments.

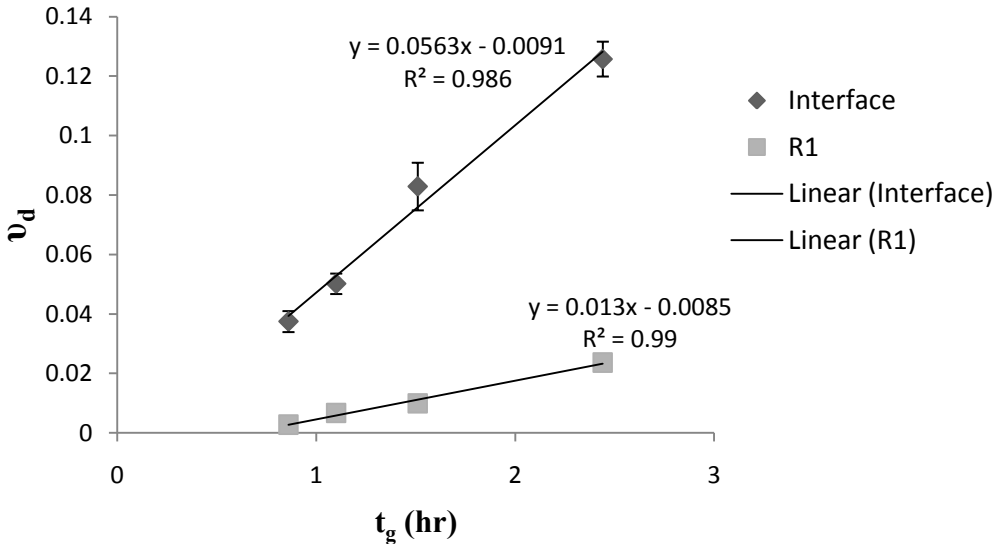

Figure 23: Dust volumetric fraction at τ=1.5

In order to determine the critical dust volume fraction, a fixed bed filtration experiment is performed. During fixed bed filtration that is without granular withdrawal, the bed continuously accumulates dust. The filtration overall efficiency eventually begins to drop as accumulation increases. The accumulation level reached when efficiency drops, marks the

critical dust volume fraction. **Figure 24** shows the result of the fixed bed experiment and the critical dust volume fractions.

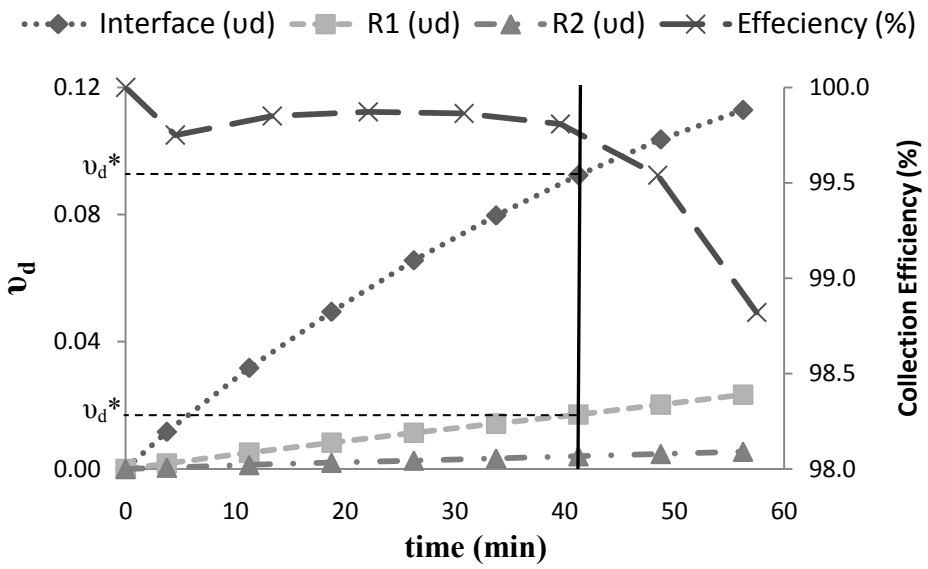

Figure 24: Dust fraction and collection efficiency vs. time for fixed bed filtration

Using the linear relationships in **Figure 23** the critical granular residence time can be estimated. **Table 7** below shows the critical dust volume fraction and granular residence time.

Table 7: Critical dust volume fraction

	Interfacial Region	**Region R1**
Critical dust volume fraction (υ_d*)	0.096 ± 0.003	0.0174 ± 0.0003
Critical granular residence time (t_g*)	1.87 ± 0.05 hr	1.99 ± 0.02 hr

Thus, the filter has to be operated below the lower critical granular residence time of 1.87 ± 0.05 hr. This value concurs with the results of the moving bed experiments, as it lies between the high and low efficiency experiments. Operating above the critical residence time would result in decreasing efficiency over time.

In the case of pyrolysis hot filtration, it is desired to have minimum char accumulation inside the filter bed, in order to avoid secondary reactions or "coking" between the hot vapors and the collected char. **Figure 25** shows the amount of char accumulation inside the filter's bed as a function of granular residence time.

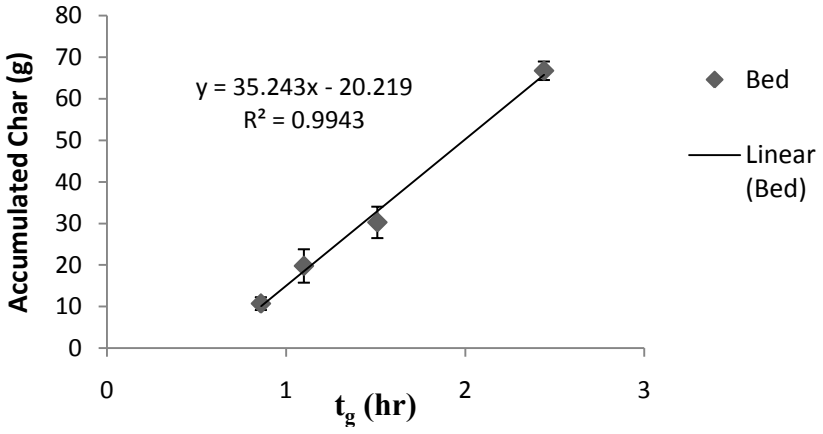

Figure 25: Accumulated char in the filter's bed at τ=1.5

Extending the linear line to zero accumulation, the granular residence time would be $t_{g(min)}$ = 0.57 hr. However, it is speculated that the accumulation line would change its slope to follow the x-axis asymptote, until reaching the origin, which is almost impossible to reach a zero residence time and accumulation in an experimental setting. The linear correlation in the figure above would be a useful tool in identifying the operational condition to minimize accumulation in the MBGF for hot gas filtration.

CHAPTER 5. CONCLUSIONS

The aim of this research was to understand the effect of granular flow rate on the collection of char within the moving bed filter. Such assessment would provide a better understanding of the operational and design requirement for fast pyrolysis hot gas filtration. Based on experimental results several conclusions can be made.

The interfacial region is capable of holding more char while causing less increase in pressure drop compared to the downcomer region. This is due to fact that the interfacial region has larger void volume fraction.

In order to properly assess the filtration efficiency of a moving bed filter, the filter must be operated for a time period beyond the granular residence time.

The MBGF is capable of filtering pyrolysis char at high efficiency, i.e. above 99% in ambient conditions. It is identified that there exists a critical granular residence time t_g*. Operating the MBGF at a granular residence time t_g higher than t_g* would cause the filter to lose efficiency over time. Whereas operating below the critical value would maintain the filter's high efficiency. Granular flow rate has no significant effect on filtration efficiency for $t_g<t_g$*.

The dust accumulation within the MBGF reaches steady state for $t_g<t_g$*. On the other hand, the for $t_g>t_g$* the filter continues to accumulate char over time suggesting a "clogging" of the filter.

Most of the char accumulation occurs in the interfacial region, with filtration efficiency above 80%. While the downcomer region is less effective in collecting dust on the granular surface due to the lower Stokes number in that region, it appears to be entailed in achieving very high overall efficiency.

Slow withdrawal of collected char causes the filter to accumulate more char over time which leads to "clogging" of the filter, characterized by critical dust volume fraction υ_d*. Critical dust volume fraction for each region is determined by performing a fixed bed filtration test. The corresponding critical granular residence time is then estimated from the relationship of dust volume fraction υ_d versus granular residence time of the MBGF experiments. A critical residence time tg* value of 1.87 hr was estimated for the investigated char feed rate.

The linear relationship between dust accumulation and granular residence time would be a useful tool in determining the $t_{g(min)}$ at which dust accumulation would be minimum. However it is recommended to investigate the effect of operating at $t_{g(min)}$ on collection efficiency, as fast granular movement could induce dust re-entrainment.

BIBLIOGRAPHY

1. *Energy Policy Act of 2005*, U.S.D.O. Energy, Editor. 2005, Federal Energy Management Program: Washington.
2. Brown, R.C., *Biorenewable resources engineering new products from agriculture*. 2003, Ames: Iowa State Press.
3. Agblevor FA, S.J., Johnson DK. . *Pyrolysis char catalyzed destabilization of biocrude oils*. in *AIChE National Meeting*. 1997.
4. Peukert, W. and C. Wadenpohl, *Industrial separation of fine particles with difficult dust properties.* Powder Technology, 2001. **118**(1-2): p. 136-148.
5. Lehtovaara, A. and W. Mojtahedi, *Ceramic-filter behavior in gasification.* Bioresource Technology, 1993. **46**(1-2): p. 113-118.
6. Shi, H., *Similitude modeling and experiments on a moving bed granular filter*, in *Mechanical Engineering*. 2002, Iowa State University: Ames.
7. Smid, J., et al., *Granular moving bed filters and adsorbers (GM-BF/A) - Patent review: 1970-2000.* Advanced Powder Technology, 2005. **16**(4): p. 301-345.
8. Soo, S.-C., *Empirical model optimization of a moving bed granular filter for particulate removal*, in *Mechanical Engineering*. 2002, Iowa State University: Ames.
9. Ritzert, J.A., *Factors influencing the efficiency of a moving bed granular filter*, in *Mechanical Engineering*. 2004, Iowa State University: Ames.
10. Huisenga, M., *Experimental assessment of the efficiency of a moving bed granular filter using a single particle counter*, in *Energy Technology*. 2006, Royal Institute of Technology: Stockholm, Sweden.

11. Brown, R.C., et al. *Design of a moving bed granular filter for biomass gasification*. in *Proceeding of the Progress in Thermochemical Biomass Conversion Conference*. 2000. Tyrol, Austria.

12. Newby, R.A., et al., *Status of Westinghouse hot gas filters for coal and biomass power systems.* Journal of Engineering for Gas Turbines and Power, Transactions of the ASME, 1999. **121**(3): p. 401-408.

13. Saxena, S.C., R.F. Henry, and W.F. Podolski, *Particulate Removal From High-Temperature, High-Pressure Combustion Gases.* Progress in Energy and Combustion Science, 1985. **11**(3): p. 193-251.

14. Jordan, S., et al., *Experiences with crossflow granular bed filter.* Chemical Engineering Technology, 1988. **60**(1): p. 34-35.

15. Ritzert J.A., R.C.B., Jerod Smeenk, *Filtration Efficiency of a Moving Bed Granular Filter*, in *Science in Thermal and Chemical Biomass Conversion*. 2004: Victoria, B.C., Canada.

16. Tien, C., *Granular Filtration of Aerosols and Hydrosols*. 1989: Butterworths.

17. Brown, R.C., *Air Filtration An Integrated Approach to the Theory and Applications of Fibrous Filters*. 1993: Pergamon Press.

18. C. Tien, B.V.R., *Granular Filtration of Aerosols and Hydrosols*. First Edition ed. 2007: Elsevier.

19. Freidlander, S.K., *Smoke, Dust, and Haze*. second ed. 2000: Oxford University Press.

20. Zevenhoven, C.A.P., K.R.G. Hein, and B. Scarlett, *Moving granular bed filtration with electrostatic enhancement for high-temperature gas clean-up.* Filtration and Separation, 1993. **30**(6): p. 550-553.

21. Richard C. Flagan, J.H.S., *Fundamentals of Air Pollution Engineering*. 1988, Englewood Cliffs, New Jersey: Prentice-Hall Inc.

22. Tsubaki, J. and C. Tien, *Gas Filtration in Granular Moving Beds - An Experimental Study*. Canadian Journal of Chemical Engineering, 1988. **66**(2): p. 271-275.

23. Peukert, W. and F. Loffler, *Optimization of the separation of particles at high temperatures in granular bed filters.* Proceedings of the International Aerosol Conference, 1990: p. 724.

24. Yang, W.C., et al. *Moving granular bed filter concept for particulate removal at high temperatures and high pressures*. 1992: dagineering Foundation.

25. Kalinowski, T.W. and D. Leith, *Aerosoll Filtration By A Concurrent Moving Granular Bed: Penetration Theory.* Environmental Science and Technology, 1983. **17**(1): p. 20-26.

26. Otani, Y., K. Miyajima, and H. Emi, *Collection performance of moving granular bed filters.* Proceedings of the International Aerosol Conference, 1990: p. 733.

27. Kuo, J.T., et al., *Stagnant zones in granular moving bed filters for flue gas cleanup.* Journal of Petroleum Science & Engineering, 1998. **20**(1-2): p. 529-534.

28. Metrix, P., *Process Particle Counter Manual*. Vol. 1. 2007, Pleasanton, California.

29. Pollard, A.J.S., *Comparison of bio-oil produced in a fractionated bio-oil collection system*, in *Mechanical Engineering*. 2009, Iowa State University: Ames.

30. De, S. and P.K. Nag, *Pressure drop and collection efficiency of cyclone and impact separators in a CFB.* International Journal of Energy Research, 1999. **23**(1): p. 51-60.

APPENDIX A

Comparison of experimental in-situ pressure measurements with theoretical predictions.

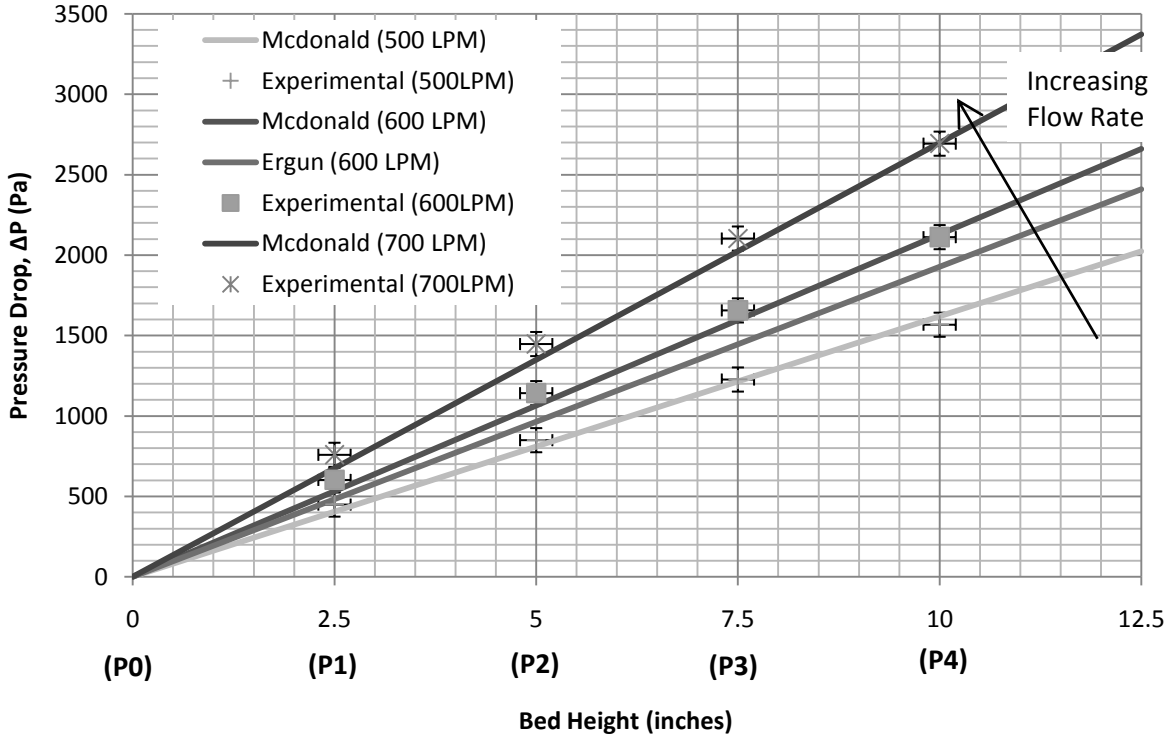

Figure B.1: Experimental and Theoretical Pressure drop across bed height in fixed bed.

Theoretical Pressure Drop Equation:

$$\frac{\Delta p}{L}\cdot\frac{Dp\cdot\rho}{G^2}\cdot\frac{\varepsilon^3}{(1-\varepsilon)} = \frac{k1}{Nre} + k2$$

$$\Delta P(\varepsilon) = \left(\frac{k1}{Nre(\varepsilon)} + k2\right)\frac{.G^2}{Dp.\rho}\frac{(1-\varepsilon)}{\varepsilon^3}L$$

Ergun equation: **k1=150** and **k2=1.75**

McDonald equation: **k1=180** and **k2=1.8**

Variables:

D (downcomer diameter) = 6 inches
Dp (particle diameter) = 2 mm
ε (void fraction) = 0.366
μ (air viscosity) = 1.98×10^{-5} kg/m.s
ρ (air density) = 1.25 kg/m^3
Q (Flow rate) = 500 LPM – 700 LPM
L (height) = 2.5-10 inches

Definitions:

$$Nre(\varepsilon) = \frac{Dp.G}{(1-\varepsilon).\mu}$$

$$G = \frac{Q.\rho}{A}$$

$$A = \frac{\pi}{4}.D^2$$

APPENDIX B

Granular Feed Rate Calibration

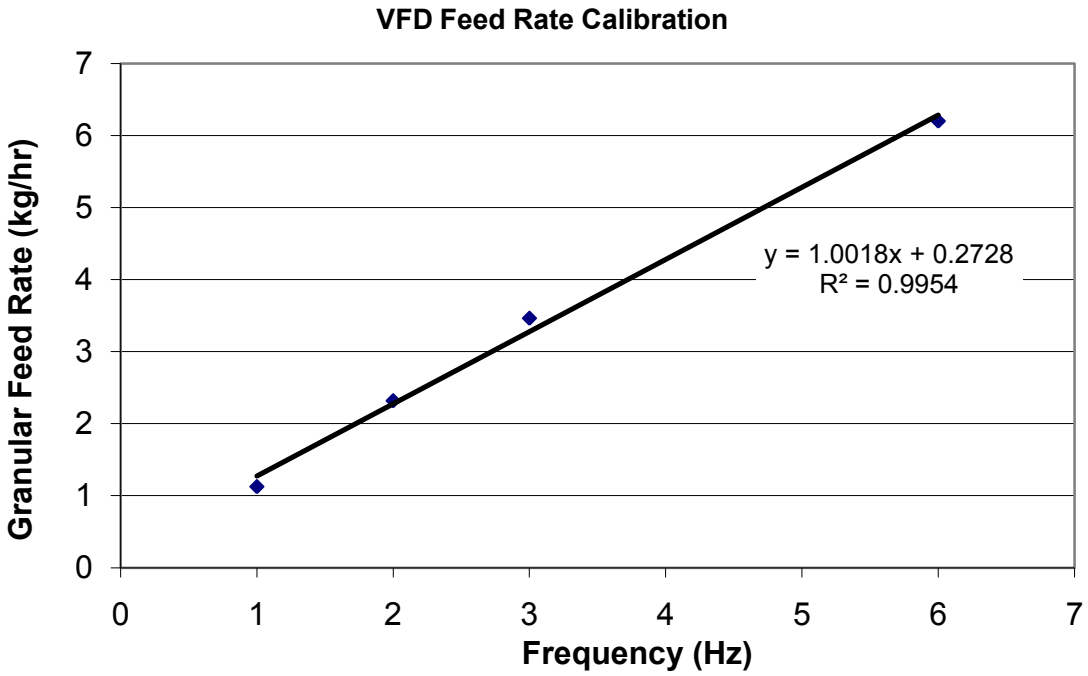

APPENDIX C

Total Uncertainty Analysis of Collection Efficiency

Total Uncertainty (U_{eff}) is has two types of uncertainties, bias (B_{eff}) and precision (P_{eff}) error. The total uncertainty can be calculated using the following equation:

$$U_{eff} = (B_{eff}^{\ 2} + P_{eff}^{\ 2})^{1/2}$$

If B_{eff} and P_{eff} has 95% confidence coverage, then U_{eff} has 95% coverage.

Bias Error calculation:

The collection efficiency is calculated as such:

$$Effeciency = 1 - \frac{C,out}{C,in}$$

Where C is the mass concentration in g/m3. The inlet concentration is calculated using the powder feeder's mass feed rate divided by the inlet flowrate. Hence:

$$Effeciency = 1 - \frac{C,out}{\left(\frac{\overset{\circ}{M},in}{\overset{\circ}{Q}air}\right)}$$

This means that the uncertainty in the efficiency value depend on three variables; outlet concentration which is read by the PPC, the inlet mass feed rate by the powder feeder, and the flow rate. The uncertainty in efficiency would be calculated as the following:

$$Beff = \sqrt{\left(\frac{\partial eff}{\partial C,out}\right)^2 \times B_{C,sout}^{\ 2} + \left(\frac{\partial eff}{\partial \overset{\circ}{M},in}\right)^2 \times B_{M,in}^{\ 2} + \left(\frac{\partial eff}{\partial \overset{\circ}{Q}air}\right)^2 \times B_{Qair}^{\ 2}}$$

Where:

$$\frac{\partial eff}{\partial C,out} = -\frac{\dot{Q}air}{\dot{M}in} \qquad \frac{\partial eff}{\partial \dot{M},in} = \frac{C,out \times \dot{Q}air}{\left(\dot{M}in\right)^2} \qquad \frac{\partial eff}{\partial \dot{Q}air} = -\frac{C,out}{\dot{M}in}$$

The bias uncertainties in the powder feeding come from error in the scale used to weigh the dust, and it also comes from the statistical standard deviation of the calibration. The uncertainty of the powder feeding is $B_{Cin} = \pm 0.1 g/\min$, which is obtained calibrating the powder feeder at 95% confidence level. The uncertainty of the inlet flow rate is $B_{Qair} = \pm 0.005 m^3/\min$, as observed on the flow controller. The uncertainty of the PPC's outlet concentration is 5% as specified by the manufacturer $B_{Cout} = \pm 2 mg/m^3$.

Variable	Test Average	Bias Uncertainty
C,out	40 mg/m^3	±2 mg/m^3 (5%)
M,in	1.71 g/min	±0.1 g/min
Q,air	600 slpm	±5 slpm
Efficiency (B_{eff})	90%-99%	± **0.02%-0.1%**

Precision Error calculation:

Precision error is calculated using the normal distribution "Two-sigma error" at 95% confidence coverage.

Example:

Efficiency (%)	Average	Standard Deviation (σ)	"Two-Sigma error" (P_{eff}) ± 1.96σ
99.55	99.487	0.146	± 0.286
99.32			
99.59			

APPENDIX D

Estimation of void fraction decrease due to char accumulation

Region	Mass of char (g)	Volume of char (m^3)	Region's volume (m^3)	Void fraction decrease
Downcomer (1 inch height)	20	2×10^{-5}	4.63×10^{-4}	0.043
Interfacial	50	5×10^{-5}	9.27×10^{-4}	0.054

Where:

Volume of char = Mass of char / char density

Char density ~ 1000 kg/m^3

Void fraction decrease = Volume of char / Region's Volume

APPENDIX E

Mass balance around the MBGF

$$\left.\frac{dm}{dt}\right)_{bed} = \dot{m}_{in} - \dot{m}_{out}$$

Where, m is the mass of dust inside the MBGF's bed, $\dot{m}_{in}$ is the constant rate of char entering the bed, and $\dot{m}_{out}$ is the rate of char leaving the bed captured on granular surface.

Assume that $\dot{m}_{out}$ is proportional to the mass of particles captured in the bed, hence:

$$\frac{dm}{dt} = \dot{m}_{in} - k \times m \qquad \text{Integrating} \Rightarrow \qquad \int_0^m \frac{dm}{km - \dot{m}_{in}} = -\int_0^t dt$$

$$\frac{1}{k}\ln\left(\frac{km - \dot{m}_{in}}{-\dot{m}_{in}}\right) = -t \qquad \Rightarrow \qquad \frac{km - \dot{m}_{in}}{-\dot{m}_{in}} = e^{-kt} \qquad \Rightarrow \qquad km - \dot{m}_{in} = -\dot{m}_{in}\, e^{-kt}$$

Therefore: $m(t) = \frac{\dot{m}_{in}}{k}(1 - e^{-kt})$

Introducing $\tau = t \times k = t/t_g$

$$m(\tau) = t_g\, \dot{m}_{in}(1 - e^{-\tau})$$

At $\tau = \infty$ (Steady State), $m(\tau = \infty) = t_g\, \dot{m}_{in}$

At $\tau = 1$, $m(\tau = 1) = t_g\, \dot{m}_{in}(0.63)$

Therefore at $\tau = 1$, m= 63% of steady state

APPENDIX F

Mass balance and efficiency calculations around bed regions

Mass balance around the interfacial region:

Definitions:

Dust loading of gas: mdg/mg

Dust loading of granules: mdG/mG

Estimation of dust loading at control surfaces of the interfacial region:

$$\left(\frac{mdG}{mG}\right)_i = \left(\frac{mdG}{mG}\right)^{Downcomer}$$

$$\left(\frac{mdG}{mG}\right)_e = \left(\frac{mdG}{mG}\right)^{Interface}$$

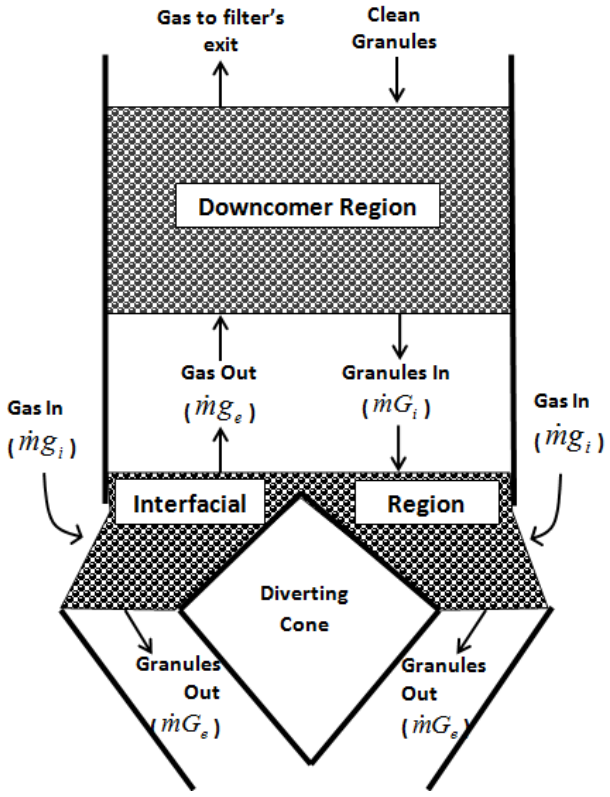

Mass balance around the interfacial region:

$$\left(\frac{mdg}{mg}\right)_i \times \dot{m}g + \left(\frac{mdG}{mG}\right)_i \times \dot{m}G = \left(\frac{mdg}{mg}\right)_e \times \dot{m}g + \left(\frac{mdG}{mG}\right)_e \times \dot{m}G$$

$$\left[\left(\frac{mdg}{mg}\right)_i - \left(\frac{mdg}{mg}\right)_e\right] \times \dot{m}g = \left[\left(\frac{mdG}{mG}\right)_e - \left(\frac{mdG}{mG}\right)_i\right] \times \dot{m}G$$

$$\left(\frac{mdg}{mg}\right)_i - \left(\frac{mdg}{mg}\right)_e = \left[\left(\frac{mdG}{mG}\right)^{Interface} - \left(\frac{mdG}{mG}\right)^{Downcomer}\right] \times \frac{\dot{m}G}{\dot{m}g}$$

Efficiency of Interface $\mathbf{Eff_I\ (\%)} = \dfrac{mdg_i - mdg_e}{mdg_i} \times 100 = \dfrac{\left.\dfrac{mdg}{mg}\right)_i - \left.\dfrac{mdg}{mg}\right)_e}{\left.\dfrac{mdg}{mg}\right)_i} \times 100$

$$= 100 \times \left[\left.\frac{mdG}{mG}\right)^{Interface} - \left.\frac{mdG}{mG}\right)^{Downcomer} \right] \times \frac{\dot{m}G}{\dot{m}g} \Big/ \left.\frac{mdg}{mg}\right)_i$$

Efficiency of Downcomer $\mathbf{Eff_D(\%)} = \dfrac{mdg_i \times (100 - Eff_I) - mdg_i \times (100 - Eff_T)}{mdg_i \times (100 - Eff_I)} \times 100$

$\mathbf{Eff_T(\%)}$: Total filter's efficiency

Example:

$\mathbf{Eff_I\ (\%)}$

$$= 100 \times \left[\left.\frac{45.1 \times 10^{-3} kg}{1.4 kg}\right)^{Interface} - \left.\frac{19 \times 10^{-3} kg}{3.3 kg}\right)^{Downcomer} \right] \times \frac{3.28 kg/hr}{0.103 kg/hr} \Big/ \left.\frac{0.103 kg/hr}{55.8 kg/hr}\right)_i$$

$$= 84\%$$

$\mathbf{Eff_D\ (\%)}$

$$= \frac{0.103 kg/hr \times (100 - 84) - 0.103 kg/hr \times (100 - 90)}{0.103 kg/hr \times (100 - 84)} \times 100$$

$$= 37.5\%$$

Appendix G

Stokes and Reynolds number calculations

Variables:

Downcomer Diameter: $Dd := 6in$

Granules Diameter $dg := 2mm$ $Rg := \frac{dg}{2}$

Char Diameter $dp := 24\mu m$ $Rp := \frac{dp}{2}$ Char Particle Density $\rho p := 1000\frac{kg}{m^3}$

Gas properties $Q := 650\frac{l}{min}$ $\mu := 1.9810^{-5}\frac{kg}{m\cdot s}$ $\rho := 1.25\frac{kg}{m^3}$ $P := 1atm$

Bed Void $\varepsilon := 0.36$

Definitions:

Downcomer Area $Ad := \left(\frac{\pi}{4}\right)\cdot Dd^2$ $Ad = 0.018m^2$

Downcomer Velocity $Ud := \frac{Q}{Ad}$ $Ud = 0.594\frac{m}{s}$

Interfacial Area $Ai := \left(\frac{\pi}{4}\right)\cdot\left[(7.5in)^2 - (6.5in)^2\right]$ $Ai = 7.094\times 10^{-3}m^2$

Interfacial Velocity $Ui := \frac{Q}{Ai}$ $Ui = 1.527\frac{m}{s}$

Gas Mean Free Path $l := \frac{\mu}{\sqrt{\frac{2\cdot P\cdot\rho}{\pi}}}$ $l = 6.973\times 10^{-8}m$

Cunningham factor $Cs := 1 + \frac{l}{Rp}\cdot\left[1.23 + 0.41e^{\left(-0.88\frac{Rp}{l}\right)}\right]$ $Cs = 1.007$

Stokes Number (Downcomer) $Std := \frac{2\cdot\rho p\cdot Rp^2\cdot Ud\cdot Cs}{9\cdot\mu\cdot Rg}$ $Std = 0.967$

Sokes Number (Interfacial) $Sti := \frac{2\cdot\rho p\cdot Rp^2\cdot Ui\cdot Cs}{9\cdot\mu\cdot Rg}$ $Sti = 2.486$

Reynolds Number (Downcomer) $Red := \frac{\rho\cdot Ud\cdot dg}{\mu\cdot(1-\varepsilon)}$ $Red = 118.274$

Reynolds Number (Interfacial) $Rei := \frac{\rho\cdot Ui\cdot 2(7.5in - 6.5in)}{\mu}$ $Rei = 4.898\times 10^3$